Dynamic Fidelity Susceptibility and its Applications to Out-of-Equilibrium Dynamics in Driven Quantum Systems

Matt Richards

A Thesis Submitted to the School of Graduate Studies in Partial Fulfilment of the Requirements for Master of Science

September 9, 2019

McMaster University
Master of Science (2019)
Hamilton, Ontario (Department of Physics and Astronomy)

TITLE: Dynamic Fidelity Susceptibility and its Applications to Out-of-Equilibrium Dynamics in Driven Quantum Systems
AUTHOR: Matt Richards (McMaster University)
SUPERVISOR: Dr. Duncan O'Dell & Dr. Erik Sørensen
NUMBER OF PAGES: 65

Abstract

In this thesis we introduce a new quantity which we call the dynamic fidelity susceptibility (DFS). We show that it is relevant to out-of-equilibrium dynamics in many-particle quantum systems, taking the problem of an impurity in a Bosonic Josephson junction, and the transverse field Ising model, as examples. Both of these systems feature quantum phase transitions in their ground states and understanding the dynamics near such critical points is currently an active area of research. In particular, sweeping a system through a quantum critical point at finite speed leads to non-adiabatic dynamics. A simple theoretical tool for describing such a scenario is the celebrated Kibble-Zurek theory which predicts that the number of excitations is related to the speed of sweep via the phase transition's critical exponents at equilibrium. Another theoretical tool, useful in describing the static properties of quantum phase transitions, is the fidelity susceptibility. Our DFS generalizes the concept of fidelity susceptibility to nonequilibrium dynamics, reproducing its results in the static limit, whilst also displaying universal scaling properties, akin to those found in Kibble-Zurek theory, in the non-adiabatic regime. Furthermore, we show that the DFS is the same quantity as the time-dependent quantum Fisher information which provides a measure of multi-partite entanglement, as well as being closely related to out-of-time-order correlators (OTOCs).

Acknowledgements

I would like to thank my supervisors Duncan O'Dell and Erik Sørensen for their eternal patience throughout the majority of my degree and their faith in my abilities as a researcher. They both provided insight and guidance towards the theories generated within this thesis. I have been incredibly fortunate to have worked with both of them as they are kind and compassionate people. My colleagues and friends (James Lambert, Anton Borissov, Ryan Plestid, Wyatt Kirkby, Jonathon Ridell, and Sriram Sundaram (in no particular order)) who work with Duncan or Erik have provided a friendly and engaging environment for me to thrive and enjoy my work. All of the fellow graduate students in the department of Physics and Astronomy have provided a warming environment in which I am happy to call home. My father has always been an inspiration for me to learn more and to question everything. My sister has always provided a listening ear to persevere through difficult times and shown me how hard work is its own reward. All of my extended family members have been incredibly supportive of my decision to pursue math and physics and have provided as much help as they can towards me achieving these goals. My best friends from Calgary have always been like brothers to me and have helped me during some of the hardest times in my life. Overall, this thesis is dedicated to my mother who always wanted me to pursue a higher education.

Contents

1 Introduction **1**

1.1 Classical Phase Transitions . . . 3
1.1.1 Landau Theory of Classical Phase Transitions . . . 4
1.1.2 Universality and Critical Exponents . . . 6
1.1.3 Homogeneity & the Scaling Hypothesis . . . 7
1.1.4 Finite Size Scaling . . . 10
1.2 Equilibrium Quantum Phase Transitions . . . 11
1.2.1 Quantum Phase Transitions . . . 12
1.2.2 Fidelity Susceptibility Applied to QPT's . . . 13
1.2.3 Zero Temperature Quantum Fisher Information . . . 16
1.3 Out-of-Equilibrium Quantum Phase Transitions . . . 17
1.3.1 Quantum Quenching and the Adiabatic Theorem . . . 17
1.3.2 Kibble-Zurek Scaling . . . 19
1.3.3 Adiabatic Perturbation Theory . . . 21

2 Dynamic Fidelity Susceptibility **25**

2.1 Dynamic Fidelity susceptibility (DFS) & the zero temperature Quantum Fisher Information . . . 25
2.1.1 Dynamic Fidelity Susceptibility in the adiabatic limit for a linear quench 27
2.1.2 Dynamic Fidelity Susceptibility in the Interaction picture . . . 29
2.1.3 Dynamic Fidelity Susceptibility and Out-of-Time Ordered Correlators 30
2.2 Application to the Transverse Field Ising model . . . 32

3 Dynamics of a Bosonic Josephson Junction coupled to an impurity atom **37**

3.1 A Bosonic Josephson Junction coupled to an impurity atom . . . 37
3.1.1 Quantum many-body Hamiltonian . . . 38
3.1.2 Equilibrium properties . . . 39
3.1.3 Universal Dynamics . . . 41

3.1.4 Dynamic Fidelity Susceptibility applied to a Bosonic Josephson Junction coupled to an impurity atom 45
3.1.5 Dynamic Fidelity Susceptibility in the Interaction Picture for a Bosonic Josephson Junction coupled to an impurity atom 50

4 Future work **53**

5 Conclusion **55**

A Solving the BJJ-impurity time dependent dynamics numerically **57**

Chapter 1

Introduction

The study of dynamics is one of the fundamental cornerstones in physics as it relates an objects motion in time to its energy (Hamiltonian). This is typically done by constructing a model to describe that energy and then solving the equations of motion governing that energy. In quantum mechanics many of the equations of motion (Schrodinger equation, Master equations, ect...) do not encapsulate all of the possible physical phenomena that could be considered in a model. As an example, by introducing a time dependence in a parameter within a constructed model, we are describing how changing this parameter in time can affect the outcome of these dynamics. From a classical perspective, including time dependence into the Hamiltonian violates the conservation of energy meaning some transfer of energy is not accurately modeled. Yet Hamiltons equations do not change their form with respect to this time dependence. The same can be said for quantum mechanics as variation in the quantum action (Feynman path integral) still arrives at the canonical time dependent Schrodinger equation regardless of how time dependence is introduced into the Hamiltonian. Part of the goal in explicitly including a time dependence into the Hamiltonian, is to accurately model the outcome of an experimenter changing a parameter in time. In this thesis, we will focus on the dynamics of quantum phase transitions which are typically treated by considering an explicit time dependence in the driving parameter.

Phase transitions are fundamental changes in the state of matter for a system of particles dependent on an order parameter and the temperature of that system [1]. Continuous second order quantum phase transitions (QPT's) are often recognized as a macroscopic change in the ground state of a system where quantum fluctuations dominate over thermal fluctuations [2]. When a system is undergoing a QPT, the quantum critical point (QCP) corresponds to a diverging correlation length which is characterized by critical exponents. These critical exponents are allocated to a notion of universality meaning they do not depend on the microscopic details of the system, rather they are determined through the universality class of the transition which is determined by inherent symmetries in the model, dimensionality, and

the range of interactions [3].

In equilibrium, universality has been one of the resounding successes of modern physics and it is utilized as a powerful tool for understanding classical [4] and quantum [2] phase transitions. For QCP's, the divergence in the correlation length is usually connected to a vanishing energy scale in the quantum system. One theoretical method for finding QCP's within quantum systems is through the fidelity susceptibility of the ground state. The fidelity susceptibility is the second order derivative of the quantum fidelity with respect to the driving parameter and it measures the sensitivity of the ground state of the system to changes in the driving parameter. The strength of the fidelity susceptibility is that it doesn't require an a priori knowledge of the local order parameter in order to determine a QCP [5, 6, 7, 8]. It has also been useful in determining finite size scaling effects along with intimate connections to quantum information [9, 10]. Through our new quantity called dynamic fidelity susceptibility (DFS), we explore similar concepts to those studied using the fidelity susceptibility in many-body quantum systems, but where they are driven out-of-equilibrium.

The DFS is defined as the second order derivative with respect to time of the overlap of the wavefunction with itself an infinitesimal time later. It is analytically equivalent to the zero temperature quantum Fisher information which is measure of multipartite entanglement [11]. Given the nature of susceptibilities, the DFS measures the sensitivity of the system to fluctuations in time. Unlike the standard fidelity susceptibility , which fundamentally assumes adiabaticity (the system is always in the ground state), the DFS allows us to us to examine truly non-equilibrium systems. Within the context of closed quantum systems initially prepared in the ground state with a time dependent driving parameter, we show the DFS has universal properties, and it is equivalent to the fidelity susceptibility in the adiabatic limit. To make the discussion concrete, we base our discussion on the Bosonic Josephson Junction coupled to an impurity atom model, along with the transverse field Ising model.

Out-of-equilibrium quantum dynamics has been a field of intense experimental [12, 13, 14, 15] and theoretical [16, 17, 18, 19] interest over the past couple decades [3]. Focusing on closed interacting models, the dynamics near quantum phase transitions can display universality [20]. One of the simplest situations is to consider a linear time dependence in the driving parameter reminiscent of the Landau-Zener problem [21]. When the order parameter is reformulated as a monotonically increasing function of time, the Kibble-Zurek mechanism provides an intuitive theoretical prediction towards calculating the critical exponents based on the rate at which the order parameter is changed [16, 17].

Adiabatic perturbation theory provides a mathematical framework for describing the universal dynamics provided one is close to the adiabatic regime [22]. However, for long and infinite range interacting models, determining critical exponents is challenging [23, 24, 25, 26], particularly when the system is driven out-of-equilibrium [27, 28, 29, 30]. We calcu-

late the time dependent dynamics of a Bosonic Josephson Junction coupled to an impurity atom (BJJ-I) and notice that the Kibble-Zurek universality breaks down for the density of defects. This is due to the inherent infinite range (all to all) interactions in the model [29]. By looking at the DFS when the BJJ-I system evolves from its many-body ground state under a linear time dependence, we directly observe universal dynamics and a connection to the zero temperature quantum Fisher information (QFI).

For pure states, the QFI is equivalent to the variance of an observable. In general, the QFI is a measure which quantifies how accurately a parameter can be estimated from the knowledge of a quantum state in an experiment [31, 32]. Astonishingly, universality in the QFI close to quantum critical points has recently been established in the equilibrium context for finite sized systems from measures of multipartite entanglement [32]. Multipartite entanglement about quantum critical points through the QFI has been a subject of much interest [33, 11, 34]. Within the Schrodinger picture, we find the DFS is exactly equivalent to the variance of the time dependent Hamiltonian thus providing a connection between multipartite entanglement and DFS. In the Interaction picture, the DFS can be represented as an Out-of-time ordered correlator (OTOC) [35, 36, 37] with similarities to Fidelity Out-of-time ordered correlators (FOTOC) [38].

OTOCs have been shown to feature an exponential growth for fast scramblers such as black holes [39, 37], and have provided a means for experimentally measuring many-body echoes [40, 41]. However, due to the decaying nature of OTOC's, experimentally differentiating between scrambling and decoherence is difficult in general for complex many-body systems [40]. When DFS is evaluated in the Interaction picture, we show that it can be represented as an OTOC indicating a connection between OTOC's and the QFI for pure states. This provides a promising result towards computationally evaluating OTOC's for driven quantum systems out-of-equilibrium.

1.1 Classical Phase Transitions

Within physics, we describe matter by analyzing it as a system of particles. Statistical mechanics has provided an accurate approach towards modeling how these systems of particles behave without knowing the individual properties for each particle within the system. In particular, one of the triumphs from this theory is in the concept of universality which predicts that changes in the state of matter (otherwise known as a phase transition) are not dependent on the microscopic details of the system. Instead they are determined by the dimensionality, range of interactions, and inherent symmetries in the model describing the system [1]. In particular, a specific set of exponents can be used to classify these phase transitions. Remarkably, many vastly different systems can share these particular exponents meaning they belong to the same universality class.

Within this section, we discuss how classical systems undergoing a phase transition can be described with Landau theory. Using this formalism, we discuss how universality arises at a critical point in which the systems changes its state of matter. Finally, this concept is shown to hold far away from the critical point through the scaling hypothesis. Each of these topics is taken with particular attention to the magnetic susceptibility in order to provide further fundamental understanding behind susceptibilities. Much of the context in this section is taken from textbooks in statistical mechanics and is used to establish the concept of universality and finding critical exponents. The main textbook is Mehran Kardars textbook "Statistical Physics of Fields" [1] and the interested reader can look further into this topic there.

1.1.1 Landau Theory of Classical Phase Transitions

When a system undergoes a drastic change at some critical temperature (T_c) due to some externally controlled variable, this is known as a Classical Phase Transition (CPT) [42]. For many classical systems, Landau's theory has had remarkable success in describing CPT's. It is a phenomenological theory based on the idea of expanding the free energy (f) as a power series in the order parameter (m) [43]

$$f(m;T) = f_0(T) + f_1(T)m + f_2(T)m^2 + O(m^3): \tag{1.1}$$

The coefficients $f_i(T)$ for $i \ 2 \ \mathbb{N}^0$ are also dependent on the underlying parameters governing the Hamiltonian. In general, this order parameter must be small ($m << 1$) on one side of the CPT and zero on the other, thus distinguishing between an ordered and disordered phase for the system.

For second order phase transitions, the order parameter changes continuously from zero starting at the critical temperature. This means that the free energy should be an even function ($f(m) = f(\ m)$) since $m \ 2 \ \mathbb{R}$. So the free energy can be expressed in even powers of the order parameter (up to the fifth order)

$$f(m;T) = am^2 + \frac{1}{2}bm^4 + O(m^6); \tag{1.2}$$

where a and b are parameters, and f_0 is removed for simplicity. By assuming $b > 0$, we are ensuring that there are local minima in the free energy for various values of m. An illustration of how this Landau free energy looks is given in Fig. (1.1).

To a first order approximation in temperature, we can write a in the form of $a(T) = a_o(T \ \ T_c)$, where $a > 0$ means $f(m;T)$ has one local minima at $m = 0$, and $a < 0$ means $f(m;T)$ has two local minima which are symmetric about $m \ 6= \ 0$. It should be noted that $T = T_c$ implies $a(T = T_c) = 0$. By minimizing Eq. (1.2), we are finding the solution to the system when it is at equilibrium and we are describing the properties of the phase transition

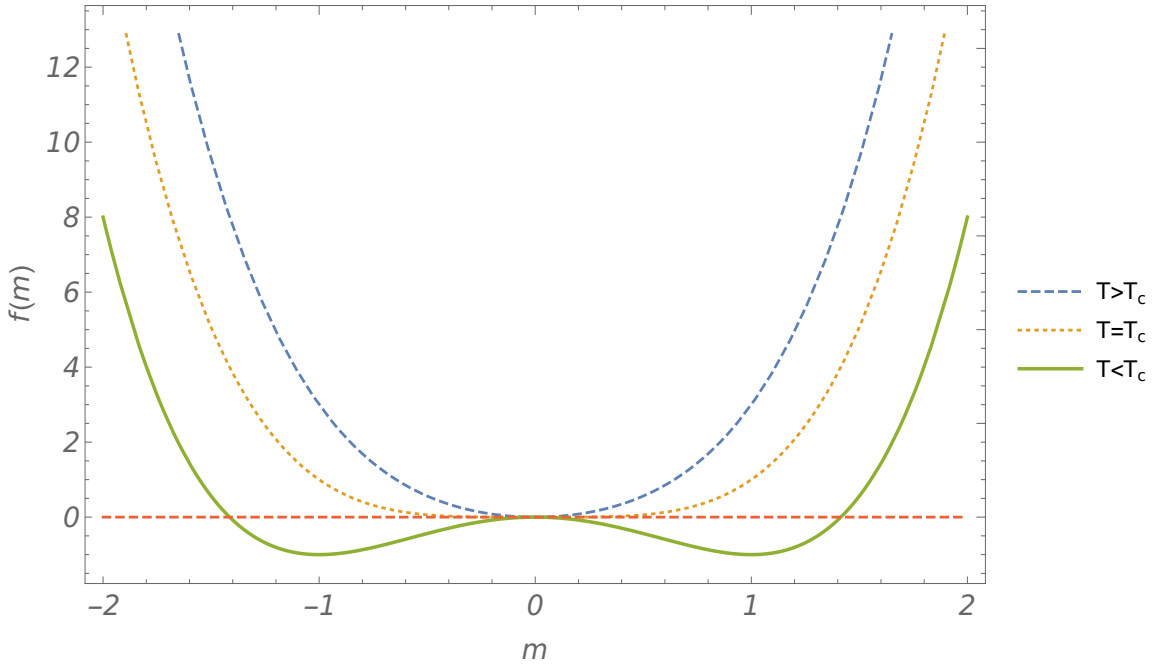

Figure 1.1: Illustration of Eq. (1.2) for various values of a and $b = 1$. As temperature decreases, the system gradually goes from one local minima at $m = 0$ to two local minima symmetric about $m = 0$. If the system were to start in equilibrium with $T > T_c$ and then slowly decrease in temperature, it would go from a stable equilibrium at $m = 0$ to an unstable equilibrium.

through the order parameter about the critical temperature. Fortunately, we can solve the order parameter at equilibrium analytically for Eq. (1.2) and the answer is

$$m(T) = \begin{cases} 0 & T > T_c; \\ \sqrt{\frac{a_0(T_c - T)}{b}} & T < T_c: \end{cases} \tag{1.3}$$

Even though we have a solution to how this system will behave in the thermodynamic limit, we have omitted a very important physical phenomena, fluctuations. We can see how prominent these fluctuations would be by considering what would happen if we started the system when $a > 0$ and then drove it to $a < 0$. Initially, it would remain in its equilibrium at $m = 0$, but a small change in m would drive the system to one of the minima.

If we consider spatial variations in the order parameter ($m(r)$) where r represents a spatial degree of freedom, we can account for the energy cost of spatial fluctuations by including a $r\,m(r)$ term into Eq. (1.2). This turns the Landau free energy into

$$f(m;a;b) \;!\; f(m(r);a;b) = \frac{s}{2}(r\,m(r))^2 + am^2 + \frac{1}{2}bm^4; \tag{1.4}$$

with some scalar value s. Solving this free energy can be quite intensive since we would need to integrate over all space to find the total energy of the system. Fortunately, we can take into account these fluctuations with a more convenient measure.

1.1.2 Universality and Critical Exponents

We can take into account spatial fluctuations near the critical point, by quantifying how prominent these fluctuations are through the correlation function. This correlation function describes how microscopic variables at different positions are related. We define the correlation function ($G(r)$) in terms of the assumed order parameter density ($m(r)$) as

$$G(r) = < m(r)m(0) > \quad < m(r) >< m(0) >; \quad \& \quad M = \left\langle \int d^d r\, m(r) \right\rangle ; \tag{1.5}$$

where $< >$ denotes ensemble average, and d is the dimensionality of the system.

Let's suppose that about the critical point, (i.e. $T = T_c$) any thermodynamic variable can be written in terms of a regular part which remains finite, plus a singular part that may diverge or have diverging derivatives [44]. Under this supposition, the singular part of the correlation function can be written in the Ornstein-Zernike form as

$$G(r) \; ! \; r^{2 \; d} \quad e^{\; \frac{r}{}} \text{ where, } \qquad \frac{T \quad T_c}{T_c} \quad : \tag{1.6}$$

The here means "has a singular part proportional to" [44] and can analytically be interpreted as "asymptotically equal".

Here, is known as the correlation length while and are known as critical exponents. The correlation length determines the length at which spatially separated correlations develop as a function of temperature (T) [1]. Notice how the correlation length diverges when T approaches T_c, indicating a phase transition in the thermodynamic limit ($N \; ! \; 1$). This divergence is characterized specifically by the critical exponent .

Inherently, a divergence in the correlation length implies singularities for other thermodynamic functions which can be characterized by particular critical exponents [1]. Some of these singular relations are illustrated in Table 1.1. Remarkably, many systems will behave similarly about critical points and share critical exponents even though their microscopic details are drastically different. This concept is known as universality and systems that share the same critical exponents are said to be in the same universality class. It is important to note that the critical exponents do not have to be the same on both sides of the critical temperature as is shown in Eq. (1.3) where $m \quad (T_c \quad T)^{\frac{1}{2}}$ when $T < T_c$ and $m \quad 0$ when $T \quad T_c$.

We can illustrate universality for thermodynamic functions, by explicitly looking at the free energy of a second order phase transition with an external field of h coupled linearly to the system. The free energy is given as

Thermodynamic Function	Critical Exponent	Singular Relation
Heat Capacity $C(T)$		$C(T)$ jT $T_c j$
Order Parameter $m(T)$		$m(T)$ $(T_c$ $T)$
Susceptibility		jT $T_c j$
Correlation Function $G(r)$		$G(r)$ r^{2} ^{d}
Correlation Length		jT $T_c j$

Table 1.1: Table of various thermodynamic functions that can experience scaling behaviour governed by the critical exponent. Inherently, the microscopic details of the model don't determine the critical exponents, rather they are determined by symmetries in the model, dimensionality (d), and the range of interactions within the model.

$$f(m; a_o; b; T; h) = a_o(T \quad T_c)m^2 + \frac{b}{2}m^4 \quad hm; \tag{1.7}$$

where $a(T) = a_o(T \quad T_c)$ and a_o is a constant. By having the free energy in this form, we are assuming the order parameter m is constant in space since there is no $r\, m(r)$ dependence. Minimizing this free energy and solving for h yields

$$h = 2am + 2bm^3: \tag{1.8}$$

This is the value of h in which the system is in equilibrium.

As an example of universality, the longitudinal susceptibility is defined as $_l{}^{1} = \lim_{h\,!\,0} \frac{dh}{dm}$ [1]. Longitudinal susceptibility is often attributed to magnetic systems where the order parameter is defined as the magnetization separating ferromagnetic and anti-ferromagnetic phases, and the external field is a magnetic field. It describes the change in magnetization with response to a field perpendicular to it [1]. By substituting in the solution for magnetization found in Eq. (1.3) into the definition of susceptibility, we arrive at

$$_l(T) = \begin{cases} \frac{1}{2jT \quad T_c j} & T > T_c; \\ \frac{1}{4jT \quad T_c j} & T < T_c: \end{cases} \tag{1.9}$$

Longitudinal susceptibility is shown in Fig. (1.2). For Longitudinal susceptibility, the critical exponent is the same on each side of the critical temperature T_c. There is however a factor of 2 difference between each side.

1.1.3 Homogeneity & the Scaling Hypothesis

Given that various thermodynamic quantities are interconnected, the critical exponents must be dependent of one another [1]. In the vicinity of a critical point, many of the more complicated critical exponents can be directly explained by a few independent exponents. We will

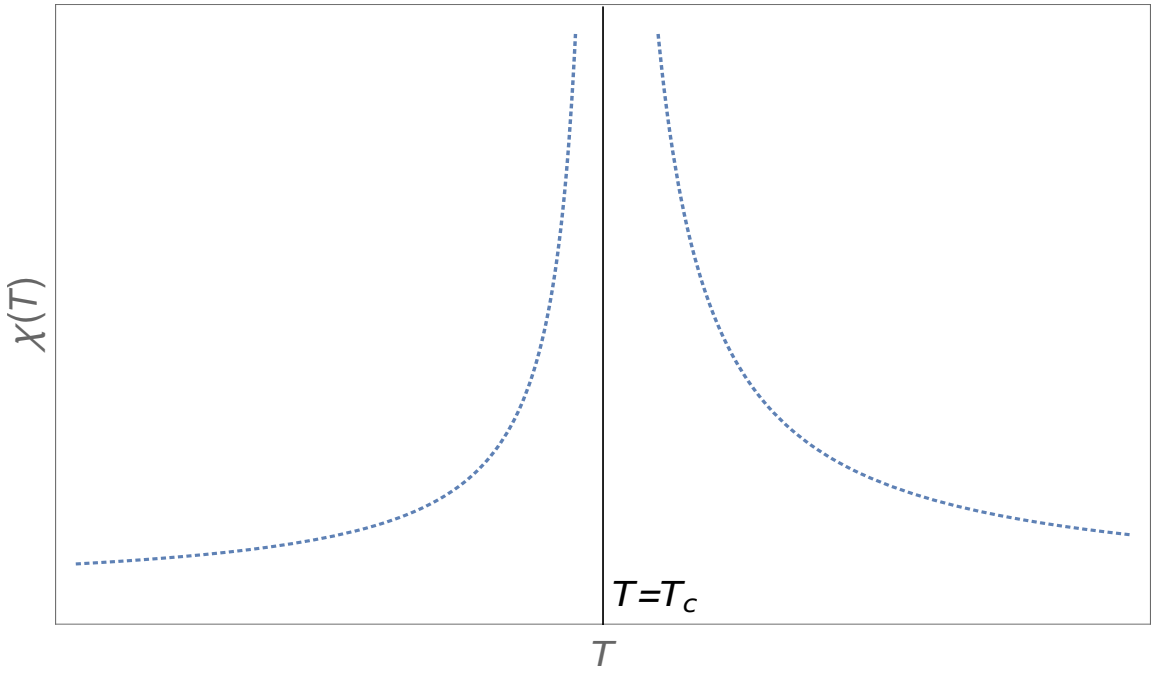

Figure 1.2: Longitudinal susceptibility ($= \lim_{h \to 0} \frac{dm}{dh}$) from Eq. (1.9) for various values of T with $a_0 = b = 1$. Longitudinal susceptibility is defined as a strictly positive value for different values of T. The critical exponent of susceptibility is given by $= 1$ for systems satisfying a free energy in the form of Eq. (1.7).

demonstrate this through the scaling hypothesis which takes a closer look around the critical point of the phase transition and looks at how various thermodynamic quantities change under a change in the correlation length [44].

One of the key assumptions for the correlation length is that it is a homogeneous function [1]. A function $g(x_1; x_2; \quad)$ is homogeneous of degree n if it can be written as

$$g(\ x_1; \ x_2; \quad) = \ ^n g(x_1; x_2; \quad); \tag{1.10}$$

for any rescaling factor . With an appropriate choice in , one of the arguments can be removed. As an example, consider the case where $= \frac{1}{x_1}$ for a homogeneous function $g(x_1; x_2; \quad)$. This gives

$$g(x_1; x_2; \quad) = x_1^n g(1; \frac{x_2}{x_1}; \quad) = x_1^n \ (\frac{x_2}{x_1}; \quad) \tag{1.11}$$

which is an equivalent way to think of homogeneity for some function [45].

In particular this can be shown when considering the singular part of the free energy defined in Eq. (1.7). For simplicity, lets rewrite $\frac{a(T)}{b} =$ and present Eq. (1.8) in a homogenous form as

$$h(\ ; m) = 2j \ j^{\frac{3}{2}} \left[\frac{m}{j \ j^{\frac{1}{2}}} + \left(\frac{m}{j \ j^{\frac{1}{2}}} \right)^3 \right] : \tag{1.12}$$

By rearranging for the order parameter, it must be in a the form of

$$m = j \ j^{\frac{1}{2}} g_1 \left(\frac{h}{j \ j^{\frac{3}{2}}} \right) ; \tag{1.13}$$

for some function g_1.

Applying the same approach to the Landau free energy given in Eq. (1.7) we arrive at

$$f(\ ; m; h) = j \ j^2 \left[\left(\frac{m}{j \ j^{\frac{1}{2}}} \right)^2 + \left(\frac{m}{j \ j^{\frac{1}{2}}} \right)^4 - \frac{h}{j \ j^{\frac{3}{2}}} \frac{m}{j \ j^{\frac{1}{2}}} \right] : \tag{1.14}$$

$$=) \quad f(\ ; m; h) = f_r(\ ; m; h) + f_s(\ ; h); \text{ where } f_s(\ ; h) = {}^2 g_2 \left(\frac{h}{j \ j^{\frac{3}{2}}} \right) ; \tag{1.15}$$

for some function g_2. In this process we have split the free energy f into a regular part f_r which remains finite as $T \ ! \ T_c$ and a singular part f_s which diverges in that limit. By choosing the value of $= \frac{a(T)}{b}$ and factoring out by a specific value, we have reduced the dependence of the free energy from three variables to two and as such eliminating the dependence on the order parameter [46].

In general, the homogeneity assumption means that the singular part of the free energy for any system takes this same form [1]

$$f_{sing}(\ ; h) = j \ j^2 \quad g_f \left(\frac{h}{j \ j} \right) : \tag{1.16}$$

The critical exponents and are the critical exponent for the heat capacity and what is called the "Gap exponent" respectively. Their values are solely dependant on the nature of the critical point [1]. Another implication of the homogeneity assumption, is that each critical exponent can be obtained directly from two independent exponents (e.g, and) [1]. As an example we can see how the susceptibility depends on and by plugging Eq. (1.16) into the definition of susceptibility giving

$$(\ ; h) = \lim_{h \ ! \ 0} \frac{@m}{@h} \quad \lim_{h \ ! \ 0} \frac{@^2 f_{sing}}{@h^2} \quad j \ j^2 \quad {}^2 \quad =) \quad = 2 \quad 2 + \quad : \tag{1.17}$$

There are many other relations comparing critical exponents to one another. Some of these are

$$+2 \quad + \quad = 2 \qquad \text{(Rushbrooke's identity);} \tag{1.18}$$

$$1 = - \qquad \text{(Widom's identity);} \tag{1.19}$$

$$2 \quad = d \qquad \text{(Josephson's identity):} \tag{1.20}$$

When the homogeneity assumption is applied to the free energy it says very little about the behaviour of correlation functions about a critical point which are key quantities in understanding how fluctuations affect a system. Instead of assuming the free energy has to be homogeneous, we can describe fluctuations through the scaling hypothesis which proposes two conditions. One is that the the correlation length is a homogeneous function, i.e.

$$(\ ; h) \quad j \ j \quad g \ \frac{h}{j \ j} \ : \tag{1.21}$$

The other condition is that close to criticality, the correlation length is the most important length scale for the system and it is solely responsible for singular contributions to thermodynamic quantities [1]. Josephson's identity Eq. (1.20) relates the critical exponent for the correlation length with other critical exponents and it is a direct consequence of the scaling hypothesis. Eq. (1.20) is known as a hyperscaling relation and any theory of critical behaviour must account for this relation in low dimensions and its breakdown for $d > 4$ [1]. Another consequence of the scaling hypothesis is that the free energy is homogeneous as well.

1.1.4 Finite Size Scaling

In reality, the thermodynamic limit is an approximation (a very good one) to our understanding of how collections of particles behave with one another. As an example, the definition of a phase transition prohibits any singularities for systems with finite sizes. Implicitly, a finite system size means that the dimensions of the system have to be finite as well. This is most adamant in experiments when the number of particles (N) can directly affect the results and numerical simulations since relevant parameters have to take on finite values. We can understand the scaling properties for systems of finite size (not in the thermodynamic limit) by applying the finite size scaling hypothesis.

The finite size scaling hypothesis states: in finite systems close to a critical point, the dominant length scales are the correlation length ( ) and the finite geometry of the system characterized by the length (L) [47]. If we consider the case of $h = 0$, we expect finite size effects to dominate when $L << (\ ; 0)$ since the correlation length can not exceed the system size [46]. If we also assume homogeneity, we can rewrite the correlation length as scaling function in the form of [47]

$$(\ ; L) = c \ (c^{\frac{1}{}} \ ; cL \ ^{1}): \tag{1.22}$$

This tells us that the inverse length is another variable that is scaled. By choosing a value of $c = L$ we arrive at

$$(\ ; L) = L \ (L^{\frac{1}{}} \ ) \tag{1.23}$$

Within the limit $L \ ! \ 1$, the correlation length should behave similarly to its form in the thermodynamic limit meaning $\lim_{x \ ! \ 1} \ (x) \ \ jxj$ since $(\ ; 0) \ \ j \ j$ from Eq. (1.21). In the other limit of $\ ! \ 0$ and $L =$ finite, the correlation length is cut off by the system size meaning $\ L$ or $\lim_{x \ ! \ 0} \ (x) \ \ $ consant. From here we can see how the susceptibility depends on the systems length L near a critical point by noting $\ ^{-}$ giving [47]

$$L^{-} \tilde{}(L^{\frac{1}{}}(T \ \ T_c)); \tag{1.24}$$

where $\tilde{}$ is a different scaling function.

1.2 Equilibrium Quantum Phase Transitions

Thermodynamics was originally formulated within the context of equilibrium and has been well establish experimentally and theoretically. In general, systems that experience a macroscopic phase transition are not in a true state of equilibrium since there has to be a difference in some external parameter driving the phase transition. However, as long as the change in these external parameters is small, the system can be well approximated to be in equilibrium. This tells us that the previously derived laws on universality and scaling can be applied experimentally.

From here, we move the discussion to quantum systems which undergo a macroscopic change in the ground state where temperature is approximated to be zero. Experimentally speaking, reaching zero temperature is impossible but very close to $T = 0$ is in fact possible. By understanding critical phenomena about $T = 0$, we can work outward to see the underlying thermodynamic and dynamic properties of the system [2].

In this section, we discuss how second order quantum phase transitions are formulated and the underlying physics driving these transitions. Next we discuss how fidelity susceptibility can be used to detect the presence of a quantum critical point and their context within the study of quantum phase transitions (QPT). Finally, we discuss how the quantum Fisher information is used as a measurable quantity to detect criticality and how it is related to multipartite entanglement.

1.2.1 Quantum Phase Transitions

Second order QPT's are defined under Hamiltonians $\hat{H}(g)$ of the form $\hat{H}(g) = \hat{H}_o + g\hat{H}_1$ where g is a dimensionless coupling [2]. g is often referred to as the driving or control parameter for the system. Analogously to the classical case, we define a critical value for the driving parameter denoted by "g_c" which is often called the quantum critical point (QCP). The QCP denotes a point at which the energy scale between the ground state and first excited state vanishes. A summary of this is given by Fig. 1.3. In Fig. 1.3 (a) the point $g = g_c$ happens at an actual level-crossing where the excited states energy becomes the ground states energy or vice versa. In general, the lowest eigenvalues will behave similarly to the illustration shown in Figure 1.3 (b). Here there is an energy gap (denoted E) between the first excited state and the ground state.

This energy gap (E) arises due to non commuting terms in the Hamiltonian. Since the temperature is taken to be zero, these non commuting components generate quantum fluctuations which dominate any thermal fluctuations. As the driving parameter reaches the QCP, the energy levels split from one another indicating the point at which quantum

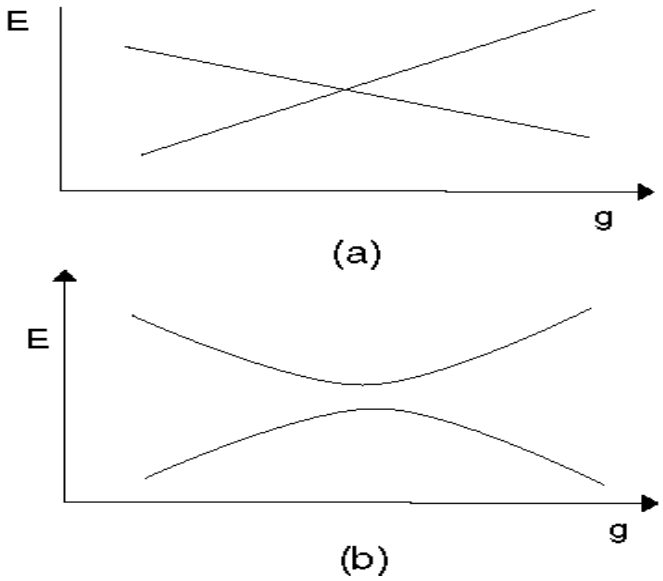

Figure 1.3: Illustration of the low energy eigenvalues (E) for $\hat{H}(g) = \hat{H}_o + g\hat{H}_1$ where g is the driving parameter. Figure (a) represents an "actual level-crossing" which can happen in the system when $[\hat{H}_o; \hat{H}_1] = 0$ and $\hat{H}_o; \hat{H}_1$ are independent of g. Figure (b) describes the more general case of an "avoided level-crossing" where $[\hat{H}_o; \hat{H}_1] \neq 0$ which ultimately leads to a gap between the excited state and the ground state denoted by E. This figure was taken from Subir Sachdev's "Quantum Phase Transitions" [2]

fluctuations are most prominent. Mathematically we can express these quantum fluctuations in terms of scaling functions and critical exponents about the QCP. In particular, the energy gap E corresponds to a diverging correlation length governed by the dynamical critical exponent z in the form of

$$E \quad ^{z} \tag{1.25}$$

We can write the singular part of the correlation length diverging as

$$^{1} \quad jg \quad g_c j \quad =) \quad E \quad J jg \quad g_c j^{z} \; ; \tag{1.26}$$

where J represents an energy scale for the characteristic microscopic coupling, and is an inverse length scale [2].

In order to understand Eq. (1.26), we can define a correlation time scale ($_t$) which is intimately related to the correlation length through the dynamical critical exponent z. This correlation time scale is defined through an on site correlation function which can be explicitly written for spin models as [48]

$$G(t; t^{0}) = h \; (r; t) \; (r; t^{0}) i \quad h \; (r; t) i h \; (r; t^{0}) i \quad =) \quad _t \quad ^{z} : \tag{1.27}$$

Physically, this correlation time scale can be related to the inverse of a characteristic frequency in the form of $! _c \quad \frac{1}{t}$ which comes from the scaling law for $E \; / \sim ! _c \quad jg \quad g_c j^{\; z}$. Intuitively, we can regard E as an energy gap between lower level energy eigenvalues. It should be noted that E is analogous to the Landau free energy in classical systems but applied to quantum systems.

1.2.2 Fidelity Susceptibility Applied to QPT's

Fidelity is defined as the overlap between an input and output state in quantum information theory [6]. In quantum physics, this overlap is defined as the transition amplitude from one state to another [6]. In general the fidelity for mixed states ($\hat{}; \hat{}^{0}$) is

$$F(\hat{}; \hat{}^{0}) = Tr(\quad \hat{}^{\frac{1}{2}} \hat{}^{0} \hat{}^{\frac{1}{2}}) \text{ and for pure states of } (\hat{}; \hat{}^{0}) \text{ is } F(\; ; \; ^{0}) = j < \quad j \; ^{0} > j : \tag{1.28}$$

Fidelity is purely a geometric quantity of a quantum state. As an example, consider a QPT induced by the level crossing of the ground state. Two states very close to the quantum critical point (QCP) but on opposite sides would have a fidelity of zero while two states far away from the critical point on one side of the QCP would have a fidelity approaching one. This simplicity allows for it's use without any knowledge of the system or the QPT [49].

If we consider a system defined as $\hat{H}(g) = \hat{H}_o + g\hat{H}_1$, its eigenstates can be found through the Schrodinger equation as

$$\hat{H}|E_n(g)\rangle = E_n(g)|E_n(g)\rangle; \tag{1.29}$$

where $E_n(g)$ are the eigenenergies set to an increasing order $E_0 < E_1 < \cdots$, and $|E_n(g)\rangle$ are the eigenstates forming an orthogonal complete basis. Within the context of QPT's the fidelity looks at how the ground state ($n = 0$ case) of the many-body system changes with an infinitesimal change in the driving parameter (g). This is explicitly written as

$$F(g) = |\langle E_0(g)|E_0(g + \ g)\rangle|: \tag{1.30}$$

By Taylor expanding the ground state fidelity (Eq. 1.30) about $g = 0$, we arrive at a more interesting form of the fidelity which formulates the overlap as a differentiable function in parameter space [6]. This is given by

$$F(g)^2 = |\langle E_0(g)|E_0(g + \ g)\rangle|^2 \quad 1 + \ g \left\langle E_0(g) \left| \frac{\partial E_0(g)}{\partial g} \right\rangle + \left\langle \frac{\partial E_0(g)}{\partial g} \right| E_0(g) \right\rangle + (\ g)^2$$
$$\left\langle \frac{\partial E_0(g)}{\partial g} \right| E_0(g) \left\rangle \left\langle E_0(g) \left| \frac{\partial E_0(g)}{\partial g} \right\rangle + \frac{1}{2}\left(\left\langle E_0(g) \left| \frac{\partial^2 E_0(g)}{\partial g^2} \right\rangle + \left\langle \frac{\partial^2 E_0(g)}{\partial g^2} \right| E_0(g) \right\rangle \right) : \right. \tag{1.31}$$

Due to normalization we require $\frac{\partial}{\partial g}(\langle E_0(g)|E_0(g)\rangle) = 0$, and properties of the fidelity tell us $F(g) \quad 1$. This inherently means that the term multiplying g is identically zero. Using the normalization condition we can express the second order derivatives in $F(g)^2$ in terms of first order derivatives as

$$\frac{d^2}{dg^2}\langle E_0(g)|E_0(g)\rangle = 0 \implies \left\langle \frac{d^2 E_0(g)}{dg^2} \right| E_0(g) \left\rangle + \left\langle E_0(g) \left| \frac{d^2 E_0(g)}{dg^2} \right\rangle = \quad 2 \left\langle \frac{dE_0(g)}{dg} \right| \left. \frac{dE_0(g)}{dg} \right\rangle : \right. \tag{1.32}$$

So

$$F(g) \quad 1 \quad \frac{(\ g)^2}{2} \ _F \text{ where} \tag{1.33}$$
$$_F(g) = \left\langle \frac{\partial E_0(g)}{\partial g} \right| \left. \frac{\partial E_0(g)}{\partial g} \right\rangle \quad \left\langle \frac{\partial E_0(g)}{\partial g} \right| E_0(g) \left\rangle \left\langle E_0(g) \left| \frac{\partial E_0(g)}{\partial g} \right\rangle : \right. \tag{1.34}$$

$_F(g)$ is also known as the fidelity susceptibility.

Although this form is general for the fidelity susceptibility, there is a much more approachable form for second order QPT's in a perturbative form. Starting from the definition of fidelity susceptibility given in Eq. (1.34), we can use the completeness relation $\sum_n |E_n\rangle\langle E_n| = 1$ to get

$$
\begin{aligned}
{}_f(g) &= \sum_{n\neq 0} \left\langle \frac{\partial E_0(g)}{\partial g} \right\rangle E_n(g) \left\rangle \left\langle E_n(g) \right| \frac{\partial E_0(g)}{\partial g} \right\rangle - \left\langle \frac{\partial E_0(g)}{\partial g} \right\rangle E_0(g) \Big\rangle^2 \\
&= \sum_{n\neq 0}^{n} \left\langle \frac{\partial E_n(g)}{\partial g} \right\rangle E_0(g) \Big\rangle^2 :
\end{aligned}
\tag{1.35}
$$

From here, we can use the known result from perturbation theory of

$$
\langle E_n(g)|\hat{H}_I|E_0(g)\rangle = \langle E_n(g)|\frac{\partial \hat{H}}{\partial g}|E_0(g)\rangle = (E_0 \quad E_n) \left\langle E_n(g) \right| \frac{\partial E_0(g)}{\partial g} \Big\rangle : \tag{1.36}
$$

This gives the final result of

$$
{}_F(g) = \sum_{n\neq 0} \frac{|\langle E_n(g)|\frac{\partial \hat{H}}{\partial g}|E_0(g)\rangle|^2}{|E_n(g) \quad E_0(g)|^2} : \tag{1.37}
$$

By definition, fidelity susceptibility is the second order derivative of the ground state fidelity in a system. It can be thought of as a measure of the sensitivity on the ground state from the driving parameter.

Remarkably, if we focus on how fidelity susceptibility behaves about the QCP, we can arrive at various critical exponents through a scaling analysis. However there are two important properties that hold for the fidelity susceptibility which are worth noting. The first is that, if $\hat{H}$ is gapped and $\hat{H}_1$ behaves like a single particle, then ${}_F$ is an intensive quantity [6]. Second, if the system is gapped, then ${}_F$ shares the same dependence on system size as the 2^{nd} order derivative of the ground state [6]. In general, this means that Fidelity Susceptibiliy can either have a similar dependence on system size as energy, or it can have some other dependence on system size.

We can find how the system scales in each case by applying finite size scaling laws [7] and evaluating at the critical point respectively to get

$$
{}_F(\quad) \quad \begin{cases} L^{\frac{2}{}} \quad {}^{d} & (g) >> L; \\ |g \quad g_c|^{d} \quad {}^{2} & (g) << L: \end{cases} \tag{1.38}
$$

Here d is the dimension of the system, L is the length of the system, (g) is the correlation length, and g_c is the critical point [50]. It should be noted that this scaling relation doesn't hold for all systems, particularly in the thermodynamic limit [50]. Overall the advantage that fidelity susceptibility has compared to Landau's theory of phase transitions, is that it doesn't require an a priori knowledge of the order parameter to detect the QPT. All it requires is a knowledge on the eigenstates of the system which can usually be found through numerical diagonalization. Alternatively, fidelity susceptibility can also represent a universal function (Y) in the form of

$$\frac{F(\ _{max};L)\quad F(\ ;L)}{F(\ ;L)} = Y(L^{\frac{1}{}}(\quad\ _{max})); \tag{1.39}$$

where $_{max}$ is the local maximum of fidelity susceptibility.

For convenience later on, it is important define the notion of a generalized fidelity susceptibility ($_m(\ )$) [51] given as

$$_m(g) = \frac{1}{L^d}\ \underset{n\neq 0}{X}\ \frac{hE_n(g)j\frac{@\hat{H}}{@g}jE_0(g)i}{(E_n(g)\quad E_0(g))^m}: \tag{1.40}$$

When $m = 2$, we arrive at the regular fidelity susceptibility. If we evaluate this at the critical point $g = g_c$ we can see how it will scale since the scaling dimension should follow dim[$_m$] = dim[$_f$] $z(m\quad 2)$ [22]. It should be noted that the dimensionality of the fidelity susceptibility can be observed from Eq. (1.38) and it is given as dim[$_f$] = $d\quad^{\frac{2}{}}$.

1.2.3 Zero Temperature Quantum Fisher Information

Quantum entanglement is a fundamental concept within quantum mechanics and it is a pivotal phenomena within quantum technologies. Recently, multipartite entanglement has been used to detect quantum phases and phase transitions theoretically [32] and experimentally [52, 53] through measurements of the ground state quantum Fisher information (QFI) [54] about a QCP. In a typical quantum experiment, many of the parameters during the experiment are unknown and are usually measured before and after the experiment [55]. The QFI quantifies the maximal precision in which a parameter q can be estimated from a state $\hat{}$ [32] before and after the experiment.

For systems at zero temperature and pure states in the form of $\hat{} = j\ \ ih\ \ j$, the QFI (F_Q) is given as [32]

$$F_Q = 4\mathrm{Var}[\hat{O}] = 4(h\ \ j\hat{O}\hat{O}j\ \ i\quad h\ \ j\hat{O}j\ \ i^2); \tag{1.41}$$

where $\hat{O}$ is a Hermitian operator associated with q. In simple terms, the QFI quantifies how distinguishable $\hat{}$ is from its unitary evolved form $\hat{}^{0}$ under $\hat{O}$. For an infinitesimal q with a mean value of 0, this is given as $\hat{}^{0} = e^{\ i\hat{O}q}\hat{}e^{i\hat{O}q}$ [32].

We can see how the QFI directly relates to measuring multipartite entanglement by considering a local generator in the form of $\hat{O} = \sum_{l=1}^{N}\hat{O}_l$ which has a spectrum of unit width. If $\hat{}$ describes an entangled state of N particles and the QFI satisfies

$$f_Q = \frac{F_Q}{N} > m \tag{1.42}$$

for m as some divisor of N, then $\hat{}$ is m + 1-partite entangled [32]. Importantly, for a large but finite system, the scaling of the QFI at zero temperature about a QCP can be represented as a scaling function given by

$$f_Q(L^{-1}; h) = \frac{4\mathrm{Var}[\sum_{l=1}^{N} \hat{O}_l]}{N} = {}^{d-2} \quad {}_Q(L^{-1}; {}^{\frac{1}{}}h) \tag{1.43}$$

where is the scaling dimension of $\hat{O}_l$, and the variance is taken with respect to the ground state.

It is important to note that the scaling of the zero temperature QFI is very similar to the scaling of the geometric tensor which is the fidelity susceptibility for a high-dimensional parameter space [56]. The QFI has also been observed experimentally in many-body quantum systems [57] making it a meaningful measurement. In the next section, we will see how QPT's behave when there is an explicit time dependence, in other words, when the system is driven out-of-equilibrium.

1.3 Out-of-Equilibrium Quantum Phase Transitions

From here we are going to restrict the condition that the system will remain in equilibrium during a phase transition. Instead we will focus on the dynamics of these phase transitions and how they can be modeled with an explicitly time dependent Hamiltonian. We do this by introducing the time dependence into the driving parameter which is modeling how an experimenter changes the driving parameter in time. We will also assume that the evolution remains unitary throughout the evolution meaning this is applied to closed quantum systems.

This whole discussion of driving out of equilibrium is taken with respect to the adiabatic theorem. In particular, we will be looking at how a quantum phase transition behaves when the control parameter is explicitly written as a linear function of time modeled by the rate of how fast it is changing. When this change is adiabatic (the rate of change is small), the system is effectively in equilibrium. In reality, a system is never truly adiabatic when crossing a quantum critical point since it corresponds to a diverging correlation time. Remarkably there are universal scaling laws dependent on the rate at which the driving parameter changes in what is known as Kibble-Zurek scaling. Finally, we will discuss how adiabatic perturbation theory is applied to the dynamics of quantum phase transitions and how it can accurately describe the behaviour from finite size effects.

1.3.1 Quantum Quenching and the Adiabatic Theorem

Within the context of quantum phase transitions (QPT's), quantum quenches are defined as a process in which a system is prepared in the eigenstate of one closed system $\hat{H}_o$ and is allowed to evolve in time under another system $\hat{H}_o + \hat{H}_1$ [58]. For sudden quenches, this evolution occurs instantaneously at a specific time. In contrast to a sudden quench is a slow quench where the system changes in a slow continuous manner (close to adiabatic) from

$\hat{H}_o$ to $\hat{H}_o + \hat{H}_1$. Quantum quenching is a very rich subject in many-body physics and has applications to many different fields such as thermalization [59, 60], and adiabatic quantum computation [61].

Throughout this thesis, we focus on slow quantum quenches (otherwise known as a driving protocol) initially prepared in the local ground state of a system, which pass through a quantum critical point (QCP) at zero temperature. For second order QPT's, the Hamiltonian for a many-body quantum system can be represented as $\hat{H}(g) = \hat{H}_o + g\hat{H}_1$. The change in the driving parameter (g) in a slow quench can be represented as a monotonically increasing function of time in the form of $g(t) = \frac{vt^r}{r!}$ where v determines the rate of change. When $r = 1$ we will refer to v as the quench speed or the driving speed. For simplicity, we are working with closed systems in the Schrodinger picture ensuring the dynamics are unitary throughout the evolution. The dynamics are governed by the time dependent Schrodinger equation given by

$$i\frac{\partial}{\partial t}|\psi(t)\rangle = \hat{H}(g(t))|\psi(t)\rangle. \tag{1.44}$$

We can apply any initial condition to Eq. (1.44) that we wish, but the simplest way to study the dynamics of quantum phase transitions is to set the initial wavefunction to the ground state in the form of $|\psi(t_o)\rangle = |E_0(g_o)\rangle$. Here, g_o is the initial parameter value in which the quench starts, and $|E_0(g_o)\rangle$ is the ground state of the system. It is important to note that this is an initial value problem meaning it is heavily dependent on the choice of the initial condition.

In general, many-body quantum systems usually depend on a plethora of parameters, making solving for the dynamics challenging. The adiabatic theorem is a powerful tool in understanding how these dynamics behave. It states: "if parameters are varied slowly with time, then the energy eigenvalues should just follow the values one gets as the parameters themselves change" [62]. This assumption is at the heart of how quantum systems evolve through a QCP and can be best understood in the context of the Landau-Zener problem [21]. From time dependent perturbation theory, we can also arrive at an adiabatic condition from the adiabatic theorem given by [62]

$$\frac{1}{\tau} >> \frac{\max[|\langle E_m(t)|\frac{d\hat{H}(t)}{dt}|E_0(t)\rangle|]}{\min[|E_m(t) - E_0(t)|^2]}, \tag{1.45}$$

where $|E_m(t)\rangle$ is the m^{th} eigenstate of $\hat{H}$. This can be expressed in a more convenient dimensional form by taking $E_m(t) - E_0(t) = \Delta$ and noting $\langle E_m(t)|\frac{d\hat{H}(t)}{dt}|E_0(t)\rangle \sim \frac{\partial}{\partial t}\Delta$ which gives [63]

$$\tau \frac{\partial}{\partial t}\Delta << \Delta^2. \tag{1.46}$$

This is the condition for which a system will remain adiabatic and when $\sim \frac{@}{@t}$ ^{2}, the systems is no longer adiabatic (non-adiabatic). In reality, the assumption of adiabaticity is often taken for granted [62] where many-body systems are always assumed to be in equilibrium. By explicitly modeling how far away the system is from equilibrium by including a time dependence, we can accurately model the dynamics of a QPT through the rate at which the driving parameter changes.

1.3.2 Kibble-Zurek Scaling

As a system is driven across a QCP, the dynamics will always fail to be adiabatic as the correlation time scale (otherwise known as the characteristic time scale) will always diverge close to a QCP [64]. Ultimately, this results in defects (or excitations) being generated in the nal state which have universal power laws dependent on the rate of quenching. This is what we refer to as universal dynamics, and even though the system is driven out of equilibrium, this scaling is dependent on critical exponents de ned in equilibrium [64]. These scaling laws are known as Kibble-Zurek scaling and have origins through Kibble within cosmology [65]. It was later pointed out that these scaling laws could be applied to continuous phase transitions in condensed matter systems by Zurek [66, 67]. From there, this has been generalized to the quantum case by Zurek, Dorner, and Zoller [16] and Polkovnikov [63].

To understand Kibble-Zurek scaling in the context of driven (time dependent) many-body QPT's, we need to apply the adiabatic theorem. The adiabatic condition (Eq. 1.45) tells us that if the gap between the ground state and rst excited state is smaller than the rate at which the driving parameter is varied, than there will be excitations generated [64]. Far away from the QCP, the system will generally evolve adiabatically, but very close to a QCP, the characteristic time scale diverges ($1=$) and the system can no longer follow the change in the Hamiltonian leading to non-adiabatic defects. The time at which the system transitions from an adiabatic state to a non adiabatic state ($\hat{t}$) known as the freeze out time is measured directly from the critical point. As the wavefunction approaches the critical point, it freezes as a result of the diverging correlation time and falls out of equilibrium. We can determine how $\hat{t}$ depends on the quench speed by invoking the non adiabatic condition [63]

$$\frac{@}{@t} \quad ^2; \tag{1.47}$$

while setting $\sim = 1$.

As an example, we will show how the scaling laws form for a linear quench i.e. $=$ $g \quad g_c = vt$ with a quench speed v. Using the non adiabatic condition and by assuming the freeze out time happens exactly when the system ceases to be adiabatic, we arrive at

$$\frac{@}{@t} \quad ^2 \ \& \ \frac{1}{t \ \hat{t}} \qquad \hat{t} \ j \ g \quad g_c j^{\,z} = (v\hat{t})^{\,z} \ =) \quad \hat{t} \quad v^{\,\frac{z}{z+1}}: \tag{1.48}$$

This is the Kibble-Zurek assumption and it is illustrated in Fig. 1.4 where the divergence of the relaxation time (characteristic time scale) is associated with a QCP.

We can express this in terms of a measurable quantity, the density of defects by noting the relation between the correlation length and the characteristic time scale (Eq. 1.27). By assuming there is one defect per unit domain, we can write the density of defects (n) to be

$$n \quad \frac{1}{d} \quad \frac{1}{\frac{d}{z}} \quad v^{\frac{d}{z+1}}: \tag{1.49}$$

For a quantum quench starting in the local ground state, the density of defects is de ned as the probability the system is not in the instantaneous ground state ($jE_0(\ (t))i$) i.e.

$$n = 1 \quad jh \quad (t)jE_0(\ (t))ij^2: \tag{1.50}$$

This also happens to be the excitation probability (P_{ex}), thus providing a simple form towards calculating the density of defects numerically with a linear quench prepared in the ground state. It should be noted that there is another observable quantity called the residual heat Q which is de ned and scales as

Figure 1.4: Illustration of the Kibble-Zurek machanism where the relaxation time is the characteristic time scale ($_t$) and the QCP happens at time zero. In the adiabatic regimes ($t > j\hat{t}j$), the wave function evolves adiabatically. Within the impulse regime ($t < j\hat{t}j$), the system does not evolve and the wavefunction remains in the same state [68], thus loosing track of the instantaneous ground state [64]. This gure was taken from “Quantum Phase Transitions in Transverse Field Spin Models” by Amit Dutta [64]

$$Q = \langle \psi(t)|\hat{H}(t)|\psi(t)\rangle - \langle E_0(\lambda(t))|\hat{H}(t)|E_0(\lambda(t))\rangle \propto v^{\frac{(d+z)}{z+1}}. \tag{1.51}$$

Alternatively, if we consider a non-linear quench in the form of $\lambda(t) = \frac{vt^r}{r!}$, their are appropriate scaling laws for the density of defects in the form of $n \propto v^{\frac{d}{zr+1}}$ and for the residual heat as $Q \propto v^{\frac{(d+z)}{zr+1}}$. Of more interest to us, one may ask how Kibble-Zurek scaling behaves for finite system sizes. If the system size is finite meaning there is a finite linear dimension of L, then the energy gap at the QCP is also a finite value. This means that it is possible to remain adiabatic as a wavefunction passes through the QCP. For a linear quench, any quench speed that is slower than $v \propto 1/L^{\frac{1}{\nu}+z}$ can achieve a perfectly adiabatic transition for a finite system size [64]. This identity can be found through applications of adiabatic perturbation theory which we will discuss next.

1.3.3 Adiabatic Perturbation Theory

When looking at the dynamics of quantum phase transitions, the Kibble-Zurek mechanism (adiabatic-impulse approximation) would lie at the heart of the process, while adiabatic perturbation theory would be the machinery of it. The overarching goal in this section is to derive an expression for the excitation probability to the leading order in v for a linear quench [22]. This procedure can be generalized to non-linear quenches but we work with the linear case for simplicity.

For a Hamiltonian in the form of $\hat{H} = \hat{H}_0 + \lambda(t)\hat{H}_I$, our goal is is to approximately solve the time-dependent Schrodinger equation given by Eq. (1.44). Given $\lambda(t) = vt$ lies between λ_o and λ_f, we can write the time dependent wavefunction in the instantaneous eigenbasis as

$$|\psi(t)\rangle = \sum_n a_n(t) e^{-i\theta_n(t)}|E_n(t)\rangle; \text{ where } \theta_n(t) = \int_{t_o}^{t} E_n(\tau)d\tau. \tag{1.52}$$

Here $E_n(t)$ is the n^{th} instantaneous eigenvalue for $|E_n(t)\rangle$ eigenstate. Due to the time dependence in the control parameter, there is an implicit time dependence on the eigenvalues and the eigenvectors. Substituting Eq. (1.52) into Eq. (1.44) and multiplying by $\langle E_m(t)|$ gives

$$\dot{a}_n(t) = \sum_m a_m(t)\langle E_n(t)|\frac{\partial}{\partial t}|E_m(t)\rangle e^{i(\theta_n(t) - \theta_m(t))}. \tag{1.53}$$

We can rewrite Eq. (1.53) in an integral form to get

$$a_n(t) = \int_{t_o}^{t} dt' \sum_m a_m(t')\langle E_n(t')|\frac{\partial}{\partial t'}|E_m(t')\rangle e^{i(\theta_n(t') - \theta_m(t'))}. \tag{1.54}$$

Since $\lambda(t)$ is a monotonic function of time, we can change variables from t to $\lambda(t)$ giving

$$_n( ) = \int_o^{} d\ ^0 \sum_m \ _m(^0)\langle E_n(^0)|\frac{@}{@ ^0}|E_m(^0)\rangle e^{i(_n(^0) \ _m(^0))}; \tag{1.55}$$

where

$$_n( ) = \int_o^{} d\ ^0 \frac{E_n(^0)}{\_^0}: \tag{1.56}$$

Upon careful examination of equations 1.54 and 1.55, we see there is a systematic expansion into the many-body excited states. For a linear quench, we are interested in the adiabatic limit which would suppress any transitions into these excited state [22]. We can also suppress these transitions by limiting the size of the integral domain ($j\ _f \ \ _oj$). To the rst order in time dependent perturbation theory, only the diagonal terms would survive ($m = n$) leading to the emergence of a Berry phase given by [22]

$$_n(t) = \ i\int_{t_o}^{t} dt^0\langle E_n(t^0)|\frac{@}{@t^0}|E_n(t^0)\rangle = \ i\int_o^{ (t)} d\ ^0\langle E_n(^0)|\frac{@}{@ ^0}|E_n(^0)\rangle: \tag{1.57}$$

This implies that $a_n(t) \quad a_n(0)e^{\ i\ _n(t)}$. For real Hamiltonians, the Berry phase vanishes which are speci cally the cases we are considering in this thesis.

Now we will actually apply adiabatic perturbation theory by computing the wavefunction up to a rst order correction in $\_$. Assuming the system is initially prepared in the ground state of $n = 0$, we get that $_0(0) = 1$ and $_n(0) = 0$ for all $n \neq 0$ [64]. So to leading order in $\_$ only one term survives with $m = 0$ changing equations (1.54) and (1.55) into [22]

$$_n(t) \quad \int_{t_o}^{t} dt^0\langle E_n(t^0)|\frac{@}{@t^0}|E_0(t^0)\rangle e^{i(_n(t^0) \ _0(t^0))}; \tag{1.58}$$

$$_n( ) \quad \int_o^{} d\ ^0\langle E_n(^0)|\frac{@}{@ ^0}|E_0(^0)\rangle e^{i(_n(^0) \ _0(^0))}: \tag{1.59}$$

The transition probability from state 0 to state n is de ned as $j\ _n(\ _f)j^2$. We can explicitly nd this rst through integration by parts leading to

$$\begin{aligned} _n(t_f) \quad & i\frac{\langle E_n(t)|\frac{@}{@t}|E_0(t)\rangle}{E_n(t) \quad E_0(t)} e^{i(_n(t^0) \ _0(t^0))}\Big|_{t_o}^{t_f} \\ & + \int_{t_o}^{t_f} dt^0 \frac{e^{i(_n(t^0) \ _0(t^0))}}{i(E_n(t^0) \quad E_0(t^0))} \frac{@}{@t^0}\langle E_n(t^0)|\frac{@}{@t^0}|E_0(t^0)\rangle : \end{aligned} \tag{1.60}$$

From time dependent perturbation theory we can simplify this in terms of the Hamiltonian ($\hat{H} = \hat{H}_o + \ (t)\hat{H}_I$) by

$$\langle E_n(t)|\frac{\partial}{\partial t}|E_0(t)\rangle = \frac{\langle E_n(t)|\frac{\partial \hat{H}}{\partial t}|E_0(t)\rangle}{E_n(t) - E_0(t)} = -\frac{\langle E_n(t)|\hat{H}_I|E_0(t)\rangle}{E_n(t) - E_0(t)}: \tag{1.61}$$

Using this identity, the second term in Eq. (1.60) drops out to the leading order in ϵ for a linear quench $\lambda = vt$. This means that the excitation probability (P_{ex}) can be written as

$$P_{ex} = \sum_{n\neq 0} |\alpha_n(\lambda_f)|^2 \sum_{n\neq 0} v^2 \frac{\langle E_n(\lambda)|\frac{\partial}{\partial \lambda}|E_0(\lambda)\rangle}{E_n(\lambda) - E_0(\lambda)}\Bigg|_0^{\lambda_f} \tag{1.62}$$

$$= v^2 L^d (\chi_4(\lambda_f) - \chi_4(\lambda_0)) \tag{1.63}$$

$$\sum_{n\neq 0} 2v^2 L^d \frac{\langle E_n(\lambda)|\frac{\partial}{\partial \lambda}|E_0(\lambda)\rangle}{E_n(\lambda) - E_0(\lambda))}\Bigg|_{\lambda=\lambda_0}^{\lambda=\lambda_f} \cos[\theta_{n;0}]; \tag{1.64}$$

where $\chi_4(\lambda)$ is the generalized susceptibility given in Eq. 1.40 to the fourth order, and $\theta_{n;0} = \theta_n(\lambda_f) - \theta_0(\lambda_f) - \theta_n(\lambda_0) + \theta_0(\lambda_0)$. If there are many eigenstates within the system, the fast oscillating term in Eq. (1.64) will average out to be zero [22].

In the case of a linear quench starting off in the ground state far from the critical point, and ending at the QCP ($\lambda = 0$) we can determine the finite size scaling through dimensionality arguments. It should be noted that the initial generalized fidelity is identically zero at the start of the quench given it is sufficiently far from the QCP. From the scaling laws for fidelity susceptibility given in Eq. (1.38) we can apply the relation $\dim[\chi_4] = \dim[\chi_f]$ $2z = d - \frac{2}{\nu} - 2z$ when $d < \frac{2}{\nu} + 2z$ [22]. This divergence leads to the finite size scaling of the excitation probability given as

$$P_{ex}(v) = v^2 L^d \chi_4(0) \quad v^2 L^{\frac{2}{\nu}+2z}: \tag{1.65}$$

For velocities more adiabatic than $v \quad L^{-\frac{1}{\nu z}}$ (i.e. $v < v^*$), the wavefunction becomes a perfectly adiabatic transition and the excitation probability looses universality meaning $P_{ex} \quad v^2$ [28].

It should be noted that within the thermodynamic limit, there is no such thing as a perfectly adiabatic transition since there isn't a finite gap size for the system to pass through. This analysis can be applied to any non-linear quench in a synonymous manner. Adiabatic perturbation theory can also be used to explicitly solve for the density of defects in a system but we will not discuss it here. The interested reader may refer to the paper “Universal Dynamics Near Quantum Critical Points” by Gritsev and Polkovnikov [22].

Chapter 2

Dynamic Fidelity Susceptibility

This chapter focuses on the main analytic results found within the thesis. We introduce a new quantity called dynamic delity susceptibility which generalizes the concept of delity susceptibility to the nonequilibrium dynamics. From its de nition and the time dependent Schrodinger equation, we nd it is analytically equivalent to the zero temperature quantum Fisher information. We demonstrate the convergence of DFS to the delity susceptibility for linear time dependent Hamiltonians in the adiabatic limit. Lastly, we will discuss the connection between DFS and delity out-of-time correlators (FOTOC's) [38] in the Interaction picture. The goal of this thesis is to motivate the usefulness of dynamic delity susceptibility and its possible applications to driven quantum systems.

2.1 Dynamic Fidelity susceptibility (DFS) & the zero temperature Quantum Fisher Information

We de ne the dynamic delity $F(t)$ as

$$F(t) = \langle h\ (t)|\ (t+\ t)\rangle; \tag{2.1}$$

where $\ t$ is an in nitesimal step in time for the wavefunction governed by Eq. (1.44). When compared to the quantum delity (Eq. 1.30) this is a more general form for dynamic systems and it can be directly related to the quantum delity by the appropriate driving protocol. By applying a Taylor expansion for small $\ t$ we can write $|\ (t+\ t)\rangle$ as

$$|\ (t+\ t)\rangle = |\ (t)\rangle + \ t\,|\frac{@\ (t)}{@t}\rangle + \frac{\ t^2}{2}|\frac{@^2\ (t)}{@t^2}\rangle + \ldots \tag{2.2}$$

Removing terms of order $(\ t)^3$ and plugging it into the dynamic delity squared, we get

$$F(t)^2 \quad 1 + \ t\,(h\ (t)j\frac{@\ (t)}{@t}i + h\frac{@\ (t)}{@t}j\ \ (t)i + \frac{(\ t)^2}{2}\ \ 2h\frac{@\ (t)}{@t}j\ \ (t)ih\ \ (t)j\frac{@\ (t)}{@t}i \\ + (\ h\ (t)j\frac{@^2\ (t)}{@^2t}i + h\frac{@^2\ (t)}{@^2t}j\ \ (t)i\ ) \ : \tag{2.3}$$

Due to normalization, we require $\frac{@}{@t}(h\ (t)j\ \ (t)i\ ) = 0$, and properties of the dynamic delity tell us $F(t) \quad 1$. The normalization condition automatically indicates that the term which is linear in t is zero. Using the normalization condition again, we can write the second order derivatives in time as

$$h\frac{d^2\ \ (t)}{dt^2}j\ \ (t)i + h\ \ (t)j\frac{d^2\ \ (t)}{dt^2}i = \quad 2h\frac{d\ \ (t)}{dt}j\frac{d\ \ (t)}{dt}i : \tag{2.4}$$

From here, we de ne the dynamic delity susceptibility (DFS) labeled $\ ^D_F(t)$ by

$$F(t)^2 \quad 1 \quad \frac{(\ t)^2}{2}\ \ ^D_F(t) \tag{2.5}$$

where,

$$^D_F(t) = 2\,h\frac{@\ (t)}{@t}j\frac{@\ (t)}{@t}i \quad 2h\frac{@\ (t)}{@t}j\ \ (t)ih\ \ (t)j\frac{@\ (t)}{@t}i ; \tag{2.6}$$

$$= 2\,\frac{1\ \ jh\ \ \ (t)j\ \ (t+\ t)ij^2}{(\ t)^2} : \tag{2.7}$$

The DFS is analogous to the delity susceptibility except the time dependent state $j\ \ (t)i$ replaces the ground state and time t replaces the driving parameter g.

We can write this in terms of the Hamiltonian since the equation of motion for $j\ \ (t)i$ is the time dependent Schrodinger equation

$$^D_F(t) = 2[\,h\ \ (t)j\hat{H}(t)\hat{H}(t)j\ \ (t)i\ \ jh\ \ \ (t)j\hat{H}(t)j\ \ (t)ij^2] : \tag{2.8}$$

Writing this in terms of a short hand notation,

$$^D_F(t) = 2(\ h\hat{H}^2(t)i \quad (h\hat{H}(t)i\,)^2) = 2(\ \mathrm{Var}[\hat{H}(t)]) : \tag{2.9}$$

We thus arrive at the zero temperature quantum Fisher information (QFI) for pure states [31]. The QFI in a dynamic perspective, classi es how precise interferometric measurements can be made on the wavefunction while witnessing multipartite entanglement [38, 54]. Interestingly, delity susceptibility is often interpreted as a purely geometric quantity [56], which implies there might be an analogous geometric interpretation for $^D_F(t)$. It also hints at the notion of describing dynamic multipartite entanglement [57, 54] through a geometric representation.

2.1.1 Dynamic Fidelity Susceptibility in the adiabatic limit for a linear quench

The result given for the DFS in Eq. (2.9) is completely independent of what type of quenching scheme is used. If we consider a driven quantum system undergoing a quantum phase transition (QPT) by introducing a linear time dependence in the driving parameter $\lambda(t) = vt$, we observe an intuitive result in the adiabatic limit ($v \to 0$) which is written as

$$\lim_{v\to 0} \frac{1}{v^2} \chi_F(t) = \chi_F(\lambda = vt); \quad \lambda = vt) \quad \chi_F(t) \quad v^2 \chi_f(\lambda): \tag{2.10}$$

Eq. (2.10) provides the connection between DFS and fidelity susceptibility in the static (adiabatic) limit.

In order to derive this result, we start from the differential form for dynamic fidelity susceptibility ($\chi_F(t)$) i.e.

$$\chi_F(t) = \left\langle \frac{\partial |\psi(t)\rangle}{\partial t} \middle| \frac{\partial |\psi(t)\rangle}{\partial t} \right\rangle - \left| \left\langle \frac{\partial |\psi(t)\rangle}{\partial t} \middle| \psi(t) \right\rangle \right|^2. \tag{2.11}$$

We can write $|\psi(t)\rangle$ in the instantaneous eigenbasis as

$$|\psi(t)\rangle = \sum_n c_n(t) e^{-i\theta_n(t)} |E_n(t)\rangle; \tag{2.12}$$

where

$$\theta_n(t) = \int_{t_o}^{t} E_n(t')dt'. \tag{2.13}$$

Differentiating Eq. (2.12) and taking the overlap with $|\psi(t)\rangle$ gives

$$\left\langle \psi(t) \middle| \frac{\partial |\psi(t)\rangle}{\partial t} \right\rangle = \sum_m c_m(t) e^{i\theta_m(t)} \langle E_m(t)| \left[\sum_n e^{-i\theta_n(t)} \frac{dc_n(t)}{dt} |E_n(t)\rangle \right] \tag{2.14}$$

$$i\theta_n(t) \frac{dc_n(t)}{dt} |E_n(t)\rangle + c_n(t) \frac{\partial |E_n(t)\rangle}{\partial t} \Big] \tag{2.15}$$

$$= \sum_n c_n(t) \frac{dc_n(t)}{dt} \quad i|c_n(t)|^2 \frac{d\theta_n(t)}{dt} \tag{2.16}$$

$$+ \sum_m \sum_n c_m(t) e^{i(\theta_m(t) \quad \theta_n(t))} c_n(t) \langle E_m(t)| \frac{\partial}{\partial t} |E_n(t)\rangle. \tag{2.17}$$

The time dependent Schrodinger equation then tells us

$$\frac{dc_n(t)}{dt} = \sum_m c_m(t) \langle E_n(t)| \frac{\partial}{\partial t} |E_m(t)\rangle e^{-i(\theta_m(t) \quad \theta_n(t))}. \tag{2.18}$$

Plugging this into the left most term of Eq. (2.17) gives

$$\left\langle \frac{\partial |\psi(t)\rangle}{\partial t} \middle| \frac{\partial |\psi(t)\rangle}{\partial t} \right\rangle = i \sum_n |c_n(t)|^2 \frac{d\theta_n(t)}{dt}. \tag{2.19}$$

Next we want to calculate the left hand term in Eq. (2.11). This is shown as

$$\begin{aligned}\left\langle \frac{\partial \Psi(t)}{\partial t} \middle| \frac{\partial \Psi(t)}{\partial t} \right\rangle &= \Big\langle \sum_m e^{i\theta_m(t)} \frac{d\,\alpha_m(t)}{dt}|E_m(t)\rangle - i\,\alpha_m(t)\frac{d\,\theta_m(t)}{dt}|E_m(t)\rangle + \alpha_m(t)\frac{\partial E_m(t)}{\partial t}\Big\rangle \\ &\quad \Big\langle \sum_n e^{i\,\theta_n(t)} \frac{d\,\alpha_n(t)}{dt}|E_n(t)\rangle - i\,\alpha_n(t)\frac{d\,\theta_n(t)}{dt}|E_n(t)\rangle + \alpha_n(t)\frac{\partial E_n(t)}{\partial t}\Big\rangle \\ &= \sum_m \sum_n e^{i(\theta_m(t) - \theta_n(t))}\,\delta_{n,m}\frac{d\,\alpha_m(t)}{dt}\frac{d\,\alpha_n(t)}{dt} - i\frac{d\,\alpha_m(t)}{dt}\alpha_n(t)\frac{d\,\theta_n(t)}{dt} \\ &\quad + i\,\alpha_m(t)\frac{d\,\theta_n(t)}{dt}\frac{d\,\alpha_n(t)}{dt} + \alpha_m(t)\,\alpha_n(t)\frac{d\,\theta_m(t)}{dt}\frac{d\,\theta_n(t)}{dt} \\ &\quad + \Big\langle E_m(t)\Big|\frac{\partial E_n(t)}{\partial t}\Big\rangle \frac{d\,\alpha_m(t)}{dt}\alpha_n(t) + i\,\alpha_m(t)\,\alpha_n(t)\Big(\frac{d\,\theta_m(t)}{dt} + \frac{d\,\theta_m(t)}{dt}\Big) \\ &\quad \alpha_m(t)\frac{d\,\alpha_n(t)}{dt} \qquad \alpha_m(t)\,\alpha_n(t)\Big\langle \frac{\partial E_m(t)}{\partial t}\Big|\frac{\partial E_n(t)}{\partial t}\Big\rangle :\end{aligned} \tag{2.20}$$

Note, we can rewrite $\langle \frac{\partial E_m(t)}{\partial t}|E_n(t)\rangle = -\langle E_m(t)|\frac{\partial E_n(t)}{\partial t}\rangle$ giving us this result. The simplest approach from here would be to take the limit $v \to 0$ and analyze how $\alpha_n(t)$ and $\frac{d\,\alpha_n(t)}{dt}$ behave in this limit. These quantities are explicitly calculated within the framework of adiabatic perturbation theory for a quantum quench starting in the ground state with a driving parameter which linearly depends on time [22] (i.e. $= vt$). Given $|\Psi(t_o)\rangle = |E_0(t_o)\rangle$, this implies $\alpha_0(t_o) = 1\,;\ \&\ \alpha_i(t_o) = 0\,;\ 8\, i \neq 0$. Taking the integral for both sides of Eq. (2.18) and integrating by parts gives

$$\begin{aligned}\alpha_n(t) &\approx -\int_{t_o}^{t} dt'\langle E_n(t')|\frac{\partial E_0(t')}{\partial t'}\rangle e^{i(\theta_n(t') - \theta_0(t'))} \\ &= -i\frac{\langle E_n(t')|\frac{\partial E_0(t')}{\partial t'}\rangle}{E_n(t) - E_0(t)} e^{i(\theta_n(t') - \theta_0(t'))}\Big|_{t_o}^{t} : \\ &\text{Given } \langle E_n(t)|\frac{\partial E_0(t)}{\partial t}\rangle = -v\frac{\langle E_n(t)|\hat{H}_I|E_0(t)\rangle}{E_n(t) - E_0(t)} \text{ for } \hat{H} = \hat{H}_o + vt\hat{H}_I \\ &\Rightarrow \alpha_n(t) \sim v: \text{ Likewise } \frac{d\,\alpha_n(t)}{dt} \sim v^2:\end{aligned} \tag{2.21}$$

In the limit that $v \to 0$ we can remove everything of order v^3 which reduces Eq. (2.11) to

$$\begin{aligned}\lim_{v\to 0} \mathcal{D}_F(t) &= \sum_n \frac{\langle E_n(t)|\frac{\partial E_0(t)}{\partial t}\rangle}{E_n(t) - E_0(t)}^2 (E_n(t) - E_0(t))^2\Big|_{t_o}^{t} + O(v^3) \\ &\quad v^2 \sum_n \frac{|\langle E_n(t)|\hat{H}_I|E_o(t)\rangle|^2}{(E_n(t) - E_0(t))^2}\Big|_{t_o}^{t} = v^2(\ _F(\ ) - \ _F(\ _o)):\end{aligned} \tag{2.22}$$

$$\text{Thus } \lim_{v\to 0}\frac{1}{v^2}\ \mathcal{D}_F(t) \sim \ _F(\ ) \text{ up to } O(v^3):$$

Time evolution	Heisenberg (subscript H)	Interaction (subscript I)	Schrodinger (subscript S)
State Ket	N.A	$\hat{V}_I(t)$	$\hat{H}(t)$
Observables	$\hat{H}(t)$	$\hat{H}_o$	N.A

Table 2.1: Summary of the Interaction picture, the Schrodinger picture, and Heisenberg picture, for time dependent Hamiltonians $\hat{H}(t) = \hat{H}_o + \hat{V}(t)$. It is important to understand that all these pictures here represent coordinate transformations which can conveniently model the time dependence in the Hamiltonian. Note: $\hat{V}_I(t) = e^{i\hat{H}_o t}\hat{V}(t)e^{-i\hat{H}_o t}$ and $|\ (t)i_I = e^{i\hat{H}_o t}|\ (t)i_S$

Remarkably, we arrive at the result we would expect in the adiabatic limit. This tells us that there is an interesting connection between DFS and delity susceptibility along with a direct way of analyzing how multipartite entanglement in the dynamic perspective can relate to equilibrium critical exponents for a quantum critical point. This is one of the principle results of this thesis and we numerically verify this in Section 2.2 for the transverse eld Ising model and in Section 3.1.4 for the Bosonic Josephson Junction coupled to an impurity atom.

2.1.2 Dynamic Fidelity Susceptibility in the Interaction picture

In this thesis, we represent time dependent Hamiltonians in the form of $\hat{H}(t) = \hat{H}_o + \hat{V}(t)$ where the time dependent part is explicitly separated from the non time dependent form. In the celebrated Interaction picture or Dirac picture, operators evolve in a Heisenberg way under $\hat{H}_o$ and state vectors evolve in a Schrodinger way under $\hat{V}_I(t)$ where $\hat{V}_I(t) = e^{i\hat{H}_o t}\hat{V}(t)e^{-i\hat{H}_o t}$. As a brief review, the Interaction picture can be summarized in Table 2.1. Following a similar derivation for DFS, we can arrive at an interaction picture DFS ($\overset{D}{}_{F;I}(t)$) given as

$$\overset{D}{}_{F;I}(t) = 2\,\mathrm{Var}[\hat{V}_I(t)]_I\,; \tag{2.23}$$

where the I subscript denotes the Interaction picture.

We can nd the equivalent form for $\overset{D}{}_{F;I}(t)$ in the Schrodinger picture by consider it as the second derivative of the dynamic delity in the Interaction picture i.e.

$$|h\ (t)|\ (t+\ t)i_I|^2 \quad 1 \quad \frac{(\ t)^2}{2}\ \overset{D}{}_{F;I}(t): \tag{2.24}$$

Explicitly writing out this Fidelity in the Schr odinger picture gives

$$\begin{aligned} |h\ (t)|\ (t+\ t)i_I|^2 &= |h\ (t)|_S e^{-i\hat{H}_o t}e^{i\hat{H}_o(t+\ t)}|\ (t+\ t)i_S|^2 \\ &= |h\ (t)|_S e^{i\hat{H}_o\ t}|\ (t+\ t)i_S|^2: \end{aligned} \tag{2.25}$$

This is because $|\psi(t)\rangle_I = e^{i\hat{H}_o t}|\psi(t)\rangle_S$. Expanding the exponential and $|\psi(t+\delta t)\rangle$ for $\delta t \ll 1$ up to order δt^2 gives

$$\begin{aligned}
&|\langle\psi(t)|\psi(t+\delta t)\rangle_I|^2 \quad \langle\psi(t)|_S\left(1 + i\delta t\hat{H}_o \quad \frac{(\delta t)^2}{2}\hat{H}_o^2\right) \\
&\quad |\psi(t)\rangle_S + \delta t\frac{\partial|\psi(t)\rangle_S}{\partial t} + \frac{\delta t^2}{2}\frac{\partial^2|\psi(t)\rangle_S}{\partial t^2}\Big|^2 \\
&= \quad \langle\psi(t)|_S + \delta t\frac{\partial\langle\psi(t)|_S}{\partial t} + \frac{\delta t^2}{2}\frac{\partial^2\langle\psi(t)|_S}{\partial t^2}\quad 1 \quad i\delta t\hat{H}_o \quad \frac{(\delta t)^2}{2}\hat{H}_o^2\ |\psi(t)\rangle_S \\
&\langle\psi(t)|_S\left(1 + i\delta t\hat{H}_o \quad \frac{(\delta t)^2}{2}\hat{H}_o^2\right)\ |\psi(t)\rangle_S + \delta t\frac{\partial|\psi(t)\rangle_S}{\partial t} + \frac{\delta t^2}{2}\frac{\partial^2|\psi(t)\rangle_S}{\partial t^2} \\
&= 1 + \frac{(\delta t)^2}{2}\left(2(\langle\hat{H}_o\hat{H}(t)\rangle + \langle\hat{H}(t)\hat{H}_o\rangle \quad \langle\hat{H}(t)^2\rangle \quad \langle\hat{H}_o^2\rangle \quad (\langle\hat{H}(t)\rangle \quad \langle\hat{H}_o\rangle)^2\right) :
\end{aligned} \tag{2.26}$$

Here I use the convention that $\langle\ \rangle = \langle\psi(t)|_S\ \ |\psi(t)\rangle_S$. We can simplify this by noting that

$$\mathrm{Var}[\hat{H}(t) \quad \hat{H}_o] = \langle\hat{H}_o\hat{H}(t)\rangle \quad \langle\hat{H}(t)\hat{H}_o\rangle + \langle\hat{H}(t)^2\rangle + \langle\hat{H}_o^2\rangle + (\langle\hat{H}(t)\rangle \quad \langle\hat{H}_o\rangle)^2; \tag{2.27}$$

$$\Rightarrow \quad \mathcal{D}_{F;I}(t) = 2\,\mathrm{Var}[\hat{H}(t) \quad \hat{H}_o]: \tag{2.28}$$

Thus the established relation between the Interaction picture and the Schrödinger picture for the DFS is

$$\mathcal{D}_{F;I}(t) = 2(\mathrm{Var}[\hat{V}_I(t)])_I = 2(\mathrm{Var}[\hat{H}(t) \quad \hat{H}_o]_S); \tag{2.29}$$

where the S subscript denotes the Schrödinger picture. Within the Interaction picture, $\mathcal{D}_{F;I}(t)$ can also be recast in the form of an out-of-time ordered correlator (OTOC) [35, 36, 37] for small perturbations in $\delta t \ll 1$.

2.1.3 Dynamic Fidelity Susceptibility and Out-of-Time Ordered Correlators

Out-of-time ordered correlators (OTOCs) $f(t)$ are defined as

$$f(t) = \langle\hat{W}^\dagger(t)\hat{X}\hat{W}(t)\hat{X}\rangle; \quad \text{s.t. } \hat{W}(t) = e^{i\hat{H}t}\hat{W}e^{\ i\hat{H}t}; \tag{2.30}$$

where $\hat{H}$ is a quantum many-body Hamiltonian, and $\hat{W}$ & $\hat{X}$ are two initially commuting and unitary operators [38]. OTOCs have been found to directly calculate the scrambling within a system. Quantum scrambling is "the dispersal of local information into many-body quantum entanglements and correlations distributed throughout the entire system" [40]. This scrambling phenomena has been found to show exponential divergence which is reminiscent of classical chaos in the form of

$$1 \quad \mathrm{Re}\{F(t)\} \quad e^{\ \alpha t}; \tag{2.31}$$

where $_Q$ is a quantum Lyapunov exponent that serves as a proxy for quantum chaos [38].

A speci c type of OTOC called the Fidelity out-of-time ordered correlator (FOTOC) has provided a connection between scrambling and entanglement [38]. They are expressed in the form of

$$F_G(t; \quad) = h \ (0)j\hat{W}_G^y(t)\hat{}(0)\hat{W}_G(t)\hat{}(0)j \ \ (0)i \text{ where } \hat{W}_G = e^{j \ \hat{G}}; \tag{2.32}$$

for a Hermitian operator $\hat{G}$. It is important to note that the key difference between a FOTOC and an OTOC is that a FOTOC speci cally projects onto the initial state of the system by setting $\hat{X} = \hat{}(0)$. For suf ciently small perturbations ($<<$ 1) and pure states, the FOTOC reduces to [69]

$$1 \ F_{\ G} \quad {}^2(h \ (0)j\hat{G}^2(t)j \ \ (0)i \ \ h \quad (0)j\hat{G}(t)j \ \ (0)i^2); \tag{2.33}$$

in the Heisenberg picture. FOTOC's have been applied to the Dicke model [70] showing theoretical connections between scrambling, volume-law R ényi entropy (RE), and thermalization [38]. By considering the operator $\hat{G} = \hat{V}(t)$ and projecting onto the density matrix for a pure state $\hat{}(t) = j \ (t)ih \ (t)j$ instead of the initial density matrix $\hat{}(0) = j \ (0)ih \ (0)j$, $^D_{F;I}(t)$ is directly equivalent to the FOTOC in the Interaction picture.

A FOTOC evaluated in the Interaction picture ($F_{G;I}(t; \quad)$) can be explicitly written (from the de nition provided by [38]) in the form of

$$F_{G;I}(t; \quad) = jh \ (0)je^{j\hat{H}_o t}e^{j \ \hat{G}}e^{\ i\hat{H}_o t}j \ \ (0)ij^2: \tag{2.34}$$

For a many-body time dependent Hamiltonian of the form $\hat{H}(t) = \hat{H}_o + \hat{V}(t)$, lets consider the case where $\hat{G} = \hat{V}(t)$ and $= t << 1$.

$$\begin{aligned}
&\hat{G} = \hat{V}(t) \ \& \quad = t << 1 \ =) \ F_{\ V(t);I}(t; \ t) = jh \ (0)je^{j\hat{H}_o t}e^{j \ t \ \hat{V}(t)}e^{\ i\hat{H}_o t}j \ \ (0)ij^2: \\
&F_{V(t);I}(t; \ t) = jh \ (0)je^{j\hat{H}_o t}e^{j \ t \ \hat{V}(t)}e^{\ i\hat{H}_o t}j \ \ (0)ij^2: \\
&\quad = jh \ (0)je^{j\hat{H}_o t}(1 + i(\ t)\hat{V}(t) \quad (\ t)^2(\hat{V}(t))^2 + O(\ t^3))e^{\ i\hat{H}_o t}j \ \ (0)ij^2 \\
&\quad (h \ (0)je^{j\hat{H}_o t}(1 + i(\ t)\hat{V}(t) \quad (\ t)^2(\hat{V}(t))^2)e^{\ i\hat{H}_o t}j \ \ (0)i) \\
&\quad (h \ (0)je^{j\hat{H}_o t}(1 \quad i(\ t)\hat{V}(t) \quad (\ t)^2(\hat{V}(t))^2)e^{\ i\hat{H}_o t}j \ \ (0)i):
\end{aligned} \tag{2.35}$$

So by directly evaluating the FOTOC from the standard de nition given in [38], we get

$$1 \ F_{\ V(t);I}(t; \ t) \quad (\ t)^2 \ h \ (0)je^{j\hat{H}_o t}\hat{V}(t)^2e^{\ i\hat{H}_o t}j \ \ (0)i \quad (h \ (0)je^{j\hat{H}_o t}\hat{V}(t)e^{\ i\hat{H}_o t}j \ \ (0)i)^2 : \tag{2.36}$$

This expression is very close to $^D_{F;I}(t)$ since $e^{j\hat{H}_o t}\hat{V}(t)e^{\ i\hat{H}_o t} = \hat{V}_I(t)$. However, the average is taken with respect to the initial state instead of the nal state.

When FOTOCs were first defined [38], they were established in the Heisenberg picture, within the context of a sudden quench where an interaction term is added instantaneously at some time i.e.

$$\hat{H}_{\text{sudden quench}} = \begin{cases} \hat{H}_O & t < 0; \\ \hat{H}_O + \hat{H}_I & t > 0: \end{cases} \tag{2.37}$$

If we are defining this in all generality for an explicit time dependence within the system, it no longer makes sense to take the average with the initial state. Instead, lets consider taking the average with respect to the final wave function which has evolved under the Interaction picture, i.e.

$$F_{V(t);I}(t;\ t) = \langle \psi(t)|_I e^{i\hat{H}_o t} e^{-i\ t\ \hat{V}(t)} e^{-i\hat{H}_o t} |\psi(0)\rangle\langle\psi(0)| e^{i\hat{H}_o t} e^{i\ t\ \hat{V}(t)} e^{-i\hat{H}_o t} |\psi(0)\rangle\langle\psi(0)|\psi(t)\rangle_I : \tag{2.38}$$

Next if we assume that $\hat{X} = \hat{\rho}(t) = |\psi(t)\rangle\langle\psi(t)|_I$ ($\hat{X}$ is the operator in which we are projecting the correlation onto) for a pure state, we can follow a similar derivation to that provided in Equation 2.35 to arrive at

$$1 - F_{V(t);I}(t;\ t) \quad (\ t)^2 \langle \psi(t)|_I \hat{V}_I(t)^2 |\psi(t)\rangle_I \quad (\langle \psi(t)|_I \hat{V}_I(t)|\psi(t)\rangle_I)^2 : \tag{2.39}$$

The final result is

$$2\frac{(1 - F_{V(t);I}(t;\ t))}{(\ t)^2} \quad 2\text{Var}[\hat{V}_I(t)] \qquad \chi^D_{F;I}(t) = 2\,\frac{(1 - |\langle \psi(t)|\psi(t + \ t)\rangle_I|^2)}{(\ t)^2}. \tag{2.40}$$

We can therefore conclude that dynamic fidelity susceptibility takes the form of an OTOC given as

$$\chi^D_{F;I}(t) = 2\,\frac{(1 - \langle \psi(t)|_I \hat{W}^{\dagger}_{V(t)}(t;\ t)\hat{\rho}^{\dagger}(t)\hat{W}_{V(t)}(t;\ t)\hat{\rho}(t)|\psi(t)\rangle_I)}{t^2} \tag{2.41}$$

where $\hat{W}_V(t;\ t) = e^{i\ t\ \hat{V}(t)}$, $\hat{W}_{V(t)}(t;\ t) = e^{i\hat{H}_o t}\hat{W}_V e^{-i\hat{H}_o t}$, and $\hat{\rho}(t) = |\psi(t)\rangle\langle\psi(t)|_I$. The condition for this to be an OTOC [35] is that $\hat{W}_V(t;\ t)$ and $\hat{\rho}(t)$ are initially commuting and are both unitary operators.

2.2 Application to the Transverse Field Ising model

Sachdev describes the transverse field Ising model as a quintessential system towards understanding QPT's [2]. Here we test some of our theories out for the one dimensional Transverse Field Ising model in the form of

$$\hat{H}(g) = \sum_{i=1}^{L} (S_i^x S_{i+1}^x + g S_i^z); \text{ where } S^j = \frac{\tilde{}}{2}^j; \tag{2.42}$$

with periodic boundary conditions for L spins. Within the thermodynamic limit of $L \to 1$, there are two critical points associated with $|g| = \frac{1}{2}$ between a ferromagnetic phase when $|g| < \frac{1}{2}$ and two paramagnetic phases when $|g| > \frac{1}{2}$ [2].

Here we assume a linear quench in the form of

$$g(t) = 1 \quad vt; \tag{2.43}$$

which starts deep in the paramagnetic phase at $t \to 1$, and v is the driving speed for the driving parameter. The critical exponents for this model are well known to be $z = = 1$ from the Kibble-Zurek mechanism [17] and are explicitly solved from space-time renormalization procedures [71]. The analytic solution for the wavefunction under this driving protocol can be decomposed into a set of Landau-Zener excitation probabilities where the wavefunction factorizes into a direct product of states with zero or two fermions [22]. Here we show the results for dynamic delity susceptibility by numerically solving the time-dependent Schrodinger equation through an explicit RK4 algorithm in order to avoid outlying assumptions. It should be noted that the quench of $1 \quad vt$ is chosen instead of $\frac{1}{2} \quad vt$ so that the the initial value for time $t_o = \frac{1 \quad g_o}{v}$ is further from the critical point, providing a more accurate numeric result since the time-dependent Schrodinger equation is solved as an initial value problem. Unfortunately, it also means that non-adiabatic speeds are less accurate since the initial time is closer to the critical point for those speeds.

By analyzing Fig. (2.1), we can see that there is data collapse between dynamic delity susceptibility and delity susceptibility for adiabatic quench speeds. The quantum Fisher information also behaves identically to the dynamic delity susceptibility (DFS). We take a closer look at this by analyzing Fig. (2.2) and see that there is indeed convergence to the static case. These are intuitive results one would expect when generalizing the delity susceptibility as the DFS for a driven quantum system. It naturally lends one to consider looking at dynamic delity susceptibility in the eld of out-of-equilibrium dynamics for QPT's. Unfortunately, many of the other results for DFS when applied to this model are not well established enough to consider in this thesis.

Figure 2.1: This figure is evaluated for the Transverse Field Ising model for $L = 6$ spins. Each line represents a separate quench velocity for the driving parameter $g(t)$ governed by Eq. (2.43). a) Dynamic fidelity susceptibility $\frac{D}{F}(t)/v^2$ with respect to the driving parameter $g(t)$. We calculate $\frac{D}{F}(t)$ directly from $F(t)$ by Eq. (2.7) with $t = 0.01$. b) The zero temperature quantum Fisher information $2\mathrm{Var}[\hat{H}(t)]/v^2$ is calculated directly from the time evolved wavefunction $|\psi(t)\rangle$ and is plotted as a function of the driving parameter g. Notice how the slower speeds are consistent with the results given by Eq. (2.10) indicating data collapse to the static case. The critical point occurs at $g_c = 0.5$ and the reason why the maximum of the fidelity susceptibility isn't exactly equal to the critical point is due to finite size effects.

Figure 2.2: Numerically evaluating the QFI $\frac{\mathrm{Var}[\hat{H}'(t_c)]}{v^2}$ for the Transverse Field Ising model with $L = 6$ spins. When this is compared to values of v, we can see a convergence to the appropriate value of $_F(W_c)$ indicated in Eq. (2.10). As the driving speeds become more adiabatic, the QFI fluctuates about the appropriate value for fidelity susceptibility indicating convergence.

Chapter 3

Dynamics of a Bosonic Josephson Junction coupled to an impurity atom

3.1 A Bosonic Josephson Junction coupled to an impurity atom

One of the original motivations for the work done during the M.Sc degree has been to look at the universal dynamics of the Bosonic Josephson Junction (BJJ) coupled to an impurity atom. The goal was to find a connection between a macroscopic Schrodinger cat state that emerges in the ground state and the critical exponents arising from the Quantum Phase Transition (QPT) in this model. Although there is a connection, due to the long-range interactions [72], measuring the density of defects does not lead to reliable scaling laws [28, 29]. Importantly, the scaling form is heavily dependent on when the quench ends which is fairly different compared to short-range interacting models [17]. While we were discovering this phenomena in the system, we also started looking at dynamic delity susceptibility (DFS) and found it has unique previously undiscovered phenomena.

From here we are going to apply the previously established theory for the DFS to the Bosonic Josephson Junction (BJJ) coupled to an impurity atom. This can be realized as a two-mode BEC-impurity double well system as illustrated in Figure 3.1. This system is closely related to the Dicke model [70], and is a relevant toy model towards further understanding the many-body effects associated with impurities [73, 72]. It experiences a second order QPT [74] in the ground state with critical exponents that can be extrapolated through the delity susceptibility [75]. DFS is shown to obey the adiabatic laws derived in Eq. (1.45) along with the direct connection to the quantum Fisher information (QFI). Remarkably, the DFS appears to exhibit numeric scaling laws dependent on the rate the driving parameter is changed for the BJJ-impurity model and hint at how DFS can be used to measure criticality in the dynamics of long-ranging interacting systems. The range in which these scaling laws happen lies when the system is non adiabatic meaning there is an interesting extension between DFS

Figure 3.1: Representation of the Bosonic Josephson Junction coupled to an impurity atom as a two-mode BEC-impurity double well model. The blue dots represent the Bosons and the red dot represents the impurity.

and delity susceptibility. We also apply some of the results found for DFS in the Interaction picture to this model and nd that many of the analytic results for DFS in the Interacton picture are numericaly veri ed.

3.1.1 Quantum many-body Hamiltonian

The simplest many-body Hamiltonian for the BJJ-impurity double well system is the single band two-site Bose-Hubbard model coupled with an impurity atom [74]. In the tight binding approximation, there is a direct mapping between the in nite range Ising model which has all-to-all interactions [72]. The impurity has a separate Hilbert space to the Bosons and being a single particle, its statistics do not matter. In all generality, this system is explicitly written as

$$\begin{aligned} \hat{H} &= U\,\hat{n}^2 \quad J\hat{B} \quad J^{a}\hat{A} + 2W\,\hat{n}\,\hat{m} \\ &+ \quad \hat{n} + \quad {}^{a}\,\hat{m}: \end{aligned} \tag{3.1}$$

Here the number difference operator for the impurity atom is given by $\hat{m} = \frac{\hat{a}_R^{y}\hat{a}_R \quad \hat{a}_L^{y}\hat{a}_L}{2} = \frac{\hat{M}_R \quad \hat{M}_L}{2}$ which gives the difference in occupation between the right and left well for the impurity atom. Likewise, the equivalent number difference operator for the Bosons is given by $\hat{n} = \frac{\hat{b}_R^{y}\hat{b}_R \quad \hat{b}_L^{y}\hat{b}_L}{2} = \frac{\hat{N}_R \quad \hat{N}_L}{2}$. Subscripts of R and L denote the respective operator or parameter being in the right or left well respectively. The eigenvalues of the operators are $n\ 2\ [\frac{N}{2}; \frac{N}{2}]$ where $N\ \ 2\ N$ is the total number of Bosons $N = N_R + N_L$, and $m = \frac{1}{2}$

where $M = M_R + M_L = 1$. Similarly, the hopping operators for the impurity and Bosons are respectively given as $\hat{A} = \hat{a}_L^\dagger \hat{a}_R + \hat{a}_R^\dagger \hat{a}_L$ and $\hat{B} = \hat{b}_L^\dagger \hat{b}_R + \hat{b}_R^\dagger \hat{b}_L$.

The particle interaction parameters in this Hamiltonian are U and W which are the intrawell interaction energies between two Bosons and between a Boson impurity respectively. J is the Bosonic hopping energy and $$ is the difference in zero-point single particle energies between the two wells. Likewise, J^a and ^{a} are the equivalent quantities for the impurity. We will refer to $$ and ^{a} as the "tilt" within the system.

3.1.2 Equilibrium properties

The ground state of the system $|E_0(W)\rangle$ becomes a macroscopic superposition as the coupling energy W approaches relatively large values. These values are cited to be at $W \quad 100U$,

Figure 3.2: This figure is evaluated for a system size of $N = 100$ Bosons. It compares the amplitude of the ground state energy $|\ _o|$ to the position of the Bosons (n) at $J = J^a$ and $= \ ^a = 0$ for a fixed impurity position $\hat{m} = \frac{1}{2}$. As the interaction energy between the Bosons and the impurity increases (W), what we see is that the ground state approaches an extreme superposition in the form of the NOON state given in Eq. (3.2).

$J = J^a = 0.001U$, and $\quad = 0$ [72]. When the Bosons are self interacting ($U \neq 0$), the Schrodinger cat state appears to form at large values of W. Removing the self interacting term in Eq. 3.1 still leads to the ground state approaching a macroscopic superposition of the form

$$\lim_{W \to 1} |E_0(W)\rangle \propto |n = N/2;\ m = \ 1/2\rangle + |n = \ N/2;\ m = 1/2\rangle : \tag{3.2}$$

Eq. (3.2) is only shown as a proportionality compared to a normalized cat state because there are a finite number of particles. These results are shown in Figure 3.2 where the ground state explicitly turns into two separate Gaussians for large W.

In order to gain insight into the universal dynamics of the ground state QPT within the BJJ-impurity model, the differences in zero point energy or tilts for the system (, ^{a}) are set to zero. Likewise, the Boson's self interaction term (U) is set to 0. Experimentally, this self interaction can be removed by inducing a Feshbach scattering resonance using a magnetic field [76]. The effects we are interested in are not meaningfully altered by this term [72]. Previous work has shown that a second order Z_2 spontaneous symmetry breaking QPT occurs in the ground state of the system as a function of W. This only occurs when both the tilts are set to zero since introducing them would break the Z_2 symmetry in the system [74, 75]. It was found that the critical value for this QPT occurs at $W_c = 2\sqrt{JJ^a}$. For values of $W < W_c$ the Bosons and impurity occupy each well equally ($\langle \hat{n}\rangle = \langle \hat{m}\rangle = 0$) whereas above W_c, it becomes energetically favorable for the Bosons to occupy one well and the impurity the other [75].

Next, all the energies are scaling in terms of the hopping energy for the Bosons (J) and for simplicity we set the impurity's hopping energy (J^a) to be equal to J. This provides a standard relative energy scale for each parameter. Finally, we scale all the terms involving Bosons by N effectively treating the Bosons and impurity's energy on the same scale. In particular, this stops these terms dominating the impurity hopping term in the thermodynamics limit $N \to 1$. All of these things turn Eq. (3.1) into

$$\hat{H} = \frac{1}{N}\hat{B}\hat{A} + 2\frac{W}{NJ}\hat{n}\,\hat{m}: \tag{3.3}$$

The presence of a QPT is shown in Figure 3.3 by plotting the fidelity susceptibility for the BJJ-impurity model as a function of W. Through the fidelity susceptibility, the critical exponents of $= \frac{3}{2}; z = 1$ [75] have been found numerically from the finite size scaling laws for fidelity susceptibility in Eqs. (1.38 and 1.39). The dimensionality is determined to be $d = 1$ since we are representing this scaling in Fock space.

Figure 3.3: Fidelity susceptibility as de ned in Eq. (1.37) is plotted for the BJJ-impurity model given in Eq. (3.3). The maximum of the delity susceptibility tends towards the critical value denoted by the vertical black line, as the system size increases. Each curve represents a different number of Bosons N which is effectively the system size. This is a clear indication of a QPT about the critical value $W_c = 2J$, where we set $J = J^a$. The inset of the graph shows in detail the delity susceptibility for N = 10. This indicates the delity susceptibility retains the same behaviour about a new maximum value regardless of system size.

3.1.3 Universal Dynamics

Given the Hamiltonian written in Eq. (3.3), we consider a linear quench scheme starting in the local ground state. We treat the repulsive interaction energy between the Bosons and impurity (W) as the driving parameter

$$W(t) = vt; \quad \text{where} \quad t \; 2 \; [\frac{W_o}{v}; \frac{W_f}{v}] = [t_o; t_f]; \tag{3.4}$$

with $W_o = 0$ and $W_f = 4J$. v is known as the the drive speed in the system and it determines how fast the driving parameter is changed. These initial and nal values are chosen to be far away from the critical point ($W_c = 2J$) for a suf ciently "slow" drive speed (v). The value of

Figure 3.4: The overlap $P_0(t) = |\langle \psi(t)|E_0(vt)\rangle|^2$ between the exact time evolved state and the instantaneous ground state is evaluated for a system size of $N = 50$ Bosons. $P_0(t)$ is the probability that the time dependent wave function will be in the local ground state at the equivalent value for the driving parameter $W(t) = vt$. For adiabatic processes, there is very little response to the QPT which is reflected in the smallest driving speeds. Conversely, when the drive speed is large, the system does not remain in the ground state.

$W_o = 0$ is physically significant in that the system is starting off in the ground state with no interactions and then it is driven to some final state with Boson-impurity interactions. The initial state is taken to be the ground state of Eq. (3.3) at $W_o = 0$ in the form of $|\psi(t_0 = 0)\rangle = |E_0(W_0 = 0)\rangle$. The exact final state is solved numerically with an explicit RK4 algorithm for the time dependent Schrödinger equation with the time dependent driving parameter expressed in Eq. (3.4). The explicit coupled ODE's are given in Appendix A. For sufficiently adiabatic evolution, the wave function should remain in the ground state. We find that this is indeed the case at "slower" driving speeds as shown in Fig 3.4. Conversely, there is less of a response to the ground state QPT at "fast" driving speeds and the evolution is non-adiabatic.

Through adiabatic perturbation theory, finite size effects can be shown to dominate when

quench velocities are slower than v and universality saturates to an exponential value of 2 [22]. This is due to the nite system size causing a perfectly adiabatic transition about the QCP. The value of v = $1=L^{\frac{1}{+z}}$ is analytically derived in Section 1.3.3, along with the scaling of the excitation probability $P_{ex} = 1$ jh (t)jE_0(vt)ij^2 saturating to a value of 2 for suf ciently slow drive speeds.

In Figure 3.5 we plot the scaling of the density of defects ($n_{ex}(t) = P_{ex}(t) = 1$ jh (t)jE_0(vt)ij^2) with respect to the drive speed normalized by system size. Given critical exponents of = 3=2, z = d = 1, the KZ scaling law given in Eq. (1.49) becomes $n_{ex}(t_c = \frac{W_c}{v})$ $v^{\frac{d}{z+1}} = v^{\frac{3}{5}}$.

Figure 3.5: Density of defects evaluated at the critical time $n_{ex}(t_c) = 1$ jh (tc)jE_0(vtc)ij^2 compared to the driving speed scaled with system size $\frac{v}{N}$ on a logarithmic scale for the BJJ-impurity model. Each curve represents a different number of Bosons N. Long range interactions, and nite size scaling effects contribute to a break down in the predicted Kibble-Zurek scaling laws. There is however a speci c range in which Kibble-Zurek scaling can be achieved numerically. This scaling belongs to driving velocities (v) that are in the range of v N $^{\frac{1}{z}}$ < v < v_{fast}. It is expected that Kibble-Zurek scaling will hold in the thermodynamics limit for systems with all-to-all interactions [29].

Figure 3.6: Density of defects evaluated at the critical time $n_{ex}(t_c) = 1 \quad jh \quad (t_c)jE_0(vt_c)ij^2$ compared to the driving speed v on a logarithmic scale for the BJJ-impurity model with $N = 100$ Bosons. We break down the dynamics of the QPT into three regions. The first region called the adiabatic region (left of the black dashed line) occurs when the driving speed is on the order of $v \quad N^{\frac{1}{z}}$ which for this model is $v \quad N^{\frac{5}{3}}$. In the adiabatic region the density of defects is expected to loose universality and saturates to $n_{ex}(t_c) \quad v^2$ which is given by the red line. The second region is called the non-adiabatic region (between the black and magenta dashed lines) where Kibble-Zurek scaling is supposed to hold in the non-adiabatic regime. For this model, the Kibble-Zurek scaling is expected to be $n_{ex}(t_c) \quad v^{\frac{3}{5}}$ which is presented by the green line. The final third region is called the far from equilibrium region (to the right of the magenta line) where all universality is expected to break down as the wavefunction no longer has any memory of the local ground state. The value of v_{fast} is arbitrarily chosen to fit the graph.

We find this accidentally holds when the quench ends at the critical point for specific driving speeds within a range of $1 >> v > v$. Therefore, it seems that in the thermodynamic limit $N \to 1$, this system will follow Kibble-Zurek scaling laws within a bigger range of driving speeds [29, 30]. However, this scaling requires the driving speeds be slow enough that the system isn't too far from equilibrium. Indeed, Figure 3.5 shows that the KZ scaling law does not hold for all adiabatic velocities due finite size effects [22].

Similar results have been obtained for the Lipkin-Meshkov-Glick (LMG) model [29] which belongs to the Dicke model universality class [70]. Like our model, the LMG model features all-to-all interactions. A key result from lookng at the universal dynamics of the LMG model, is that the KZ universality is heavily dependent on when the quench ends for these similar all-to-all models [29]. In contrast to short range interacting models, these universal dynamics are drastically different in that they theoretically do not depend on when the quench ends.

Indeed, analysis of the ferromagnetic spinor atomic Bose-Einstein condensate by Xue et. al. [28] breaks down the dynamics of the QPT into three distinct regions. They do this by categorizing where universality at the critical time $t_c = \frac{c}{v}$ (for some driving parameter) occurs in the system:

> Region 1 which is called the adiabatic region is for velocities of $v < v$. In this case the density of defects becomes non-universal and saturates to 2, i.e. $n_{ex}(t_c)$ v^2.
>
> Region 2 called the non-adiabatic region is for velocities of $v < v < v_{fast}$. Here we arrive at the universal Kibble Zurek scaling $n_{ex}(t_c)$ $v^{\frac{d}{z+1}}$.
>
> Region 3 being the far from equilibrium region where $v_{fast} < v$. For this, the drive speed is to fast and the density of defects saturates rapidly loosing features of universality.

We compare this analysis to our system in Figure 3.6 and find identical results. Recently, other work on the long range transverse field Ising model with power law interactions $\frac{1}{r}$ where 2 [0; 1) has found that the KZ scaling laws can exist for an experimentally realizable number of particles [30]. However, these scaling laws do break down when the interactions become infinite.

3.1.4 Dynamic Fidelity Susceptibility applied to a Bosonic Josephson Junction coupled to an impurity atom

There is an intimate relationship between the dynamic fidelity susceptibility (DFS) and -fidelity susceptibility (FS) in the adiabatic limit through Eq. (2.10). This relationship is numerically shown in Figure 3.7 (a.) through the BJJ-impurity model following the quench scheme given in Eq. 3.4. In particular, there is exact convergence with dynamic fidelity susceptibility and FS in the adiabatic limit which is the intuitive result expected. Remarkably,

the exact same results are found for the zero temperature quantum fisher information (QFI) within the adiabatic limit and this is represented in Figure 3.7 (b.). Inherently this means that multipartite entanglement has a connection to the equilibrium properties of QPTs in the adiabatic limit. The connection between the QFI and multipartite entanglement is illustrated in Section 1.2.3. One of the key strengths in recognizing the connection between QFI and DFS is that it provides a general result for analyzing multipartite entanglement under a slow quench driven out of equilibrium.

We further explore the exact convergence of the QFI in Figure 3.8 by analyzing its depen-

Figure 3.7: This figure looks at the connection between dynamic fidelity susceptibility and the quantum fisher information in the adiabatic limit. We analyze this connection through the Bosonic Josephson Junction with an impurity atom coupled to it given a system size of $N = 10$ Bosons. Each line represents a separate driving speed for the driving parameter W governed by Eq. (3.4). a) Dynamic fidelity susceptibility $\chi_F(t)/v^2$ with respect to the driving parameter W. We calculate $\chi_F(t)$ directly from $F(t)$ by Eq. (2.7) with $t = 0.001$ b) Zero temperature quantum Fisher information $2\mathrm{Var}[\hat{H}(t)]/v^2$ as a function of the driving parameter W. The variance is taken with respect to the time evolved wavefunction. Notice how the slower speeds are consistent with the results given by Eq. (2.10) indicating data collapse to the fidelity susceptibility.

Figure 3.8: Convergence of the quantum Fisher information (QFI) Var $[\hat{H}(t)]/v^2$ in the BJJ-impurity model for system sizes of $N = 100$ evaluated at the critical point. The inset shows this convergence to the Fidelity Susceptibility at $N = 10$ evaluated at the critical point. It appears that for adiabatic driving speeds, the QFI fluctuates about the appropriate value for fidelity susceptibility indicating convergence. It should be noted that for the $N = 100$ case, the driving speeds used are too fast to reflect these fluctuations but are expected to behave similarly for slower speeds. If we wanted to check for slower speeds with larger system sizes, we would need to implement parallel programming in the numerical solution to reproduce results in a reasonable time.

dence on the driving speed at the critical value of $W_c = 2J$ for the BJJ-impurity model. It appears that the numerical results initially overshoot the expected convergent value at very small v for $N = 100$ Bosons. We postulate this is due to neglecting higher order perturbations in v for the derivation of Eq. (2.10). However, by considering a smaller number of Bosons $N = 10$, we observe that the QFI appears to fluctuate about the appropriate limiting value of $_F(W_c)/2$. We expect this to occur for larger system sizes with slower speeds. Unfortunately, this requires an implementation of parallel programming to produces results in a reasonable time.

Following the quench scheme outlined in Eq. (3.4) we consider treating the DFS as a scaling quantity with velocity in Figure 3.9. Remarkably, when DFS is evaluated at the cor-

Figure 3.9: Out-of-equilibrium scaling laws for the QFI by a linear quench given in Eq. (3.4), for the BJJ-impurity model about the values of $W_{max} = \frac{t_{max}}{v} = 2:197J; 2:125J$ for $N = 100; 200$ respectively. The values considered within the linear regression lie in the non-adiabatic regime, where Kibble-Zurek scaling is expected to hold for this model. The r^2 is the coef cient of determination, indicating how accurate the linear regression is in properly modeling the data. The slope of the scaling laws seem to converge to the value of 1:6 indicating a possible data collapse in the thermodynamic limit. It is important to note that the scaling for this model occurs in the non-adiabatic regime where the Kibble-Zurek scaling is expected to hold for the density of defects as presented in Figure 3.6. Remarkably, the numerical scaling appears to be quite pronounced in this region. Not only does this provide insight into how DFS can be extended beyond its connection to regular delity susceptibility, it also indicates that the DFS or the QFI is a relevant measure towards understanding universal dynamics in long-range interacting models. This scaling depends heavily on when the quench ends (t_{max}) for this system. It would be interesting to see how DFS behaves for other short range models!

responding maximum value of W for the delity susceptibility W_{max}, we nd a clear scaling law about the driving speed. Interestingly, this scaling lies in the non-adiabatic regime, speci cally where Kibble-Zurek scaling breaks down for in nite range models [28, 29]. This means that DFS goes beyond regular delity susceptibility and can accurately model phenomena that is non-adiabatic. Hopefully this provides a promising avenue towards probing the dynamics of quantum phase transitions.

Regardless, when the QFI is interpreted as the DFS, it can be used as a measure for looking at universal dynamics of slow quenches for in nite range models. Analogously, within the adiabatic limit, the DFS or the QFI can be written as a universal function about W_{max} given by Figure 3.10 in a similar manner to Eq. (1.39). This indicates that there has to be a connection between the out-of-equilibrium dynamics observed in Figure 3.9 and the equilibrium critical exponents found for this system in the adiabatic limit.

Figure 3.10: Dynamic delity susceptibility is numerically evaluated as the QFI and it is presented as a universal nite size scaling function about the maximum value of delity susceptibility in the BJJ-impurity model (which has a critical exponent of $= \frac{3}{2}$) at $N = 100$ and $v = 2:395 \quad 10^{-5}$. The static line indicates the case where Eq. (1.39) is explicitly evaluated and the dynamic line is the equivalent form given by $(\frac{D}{F}(vt_{max}) \quad \frac{D}{F}(vt)) = \frac{D}{F}(vt)$. For a suf ciently slow driving speed, the QFI exactly matches the delity susceptibilities nite size scaling relation given by Eq. (1.39) indicating universal behaviour dependent on the driving parameter W in the adiabatic limit. This could possibly hint at describing any dynamic universal scaling laws for DFS in terms of the equilibrium critical exponents.

3.1.5 Dynamic Fidelity Susceptibility in the Interaction Picture for a Bosonic Josephson Junction coupled to an impurity atom

In this section, we numerically explore some of the relations found in Chapter 2 for dynamic fidelity susceptibility (DFS) in the Interaction picture by applying them to the BJJ-impurity model. Looking at the dynamics for this time dependent system, we start off in the ground state at $W = 0$ ($|\psi(0)\rangle = |E_0(0)\rangle$) and follow the same quench scheme outlines in Eq. (3.4). The time dependent wave functions for the Schrödinger picture ($|\psi(t)\rangle_S$) and the Interaction picture ($|\psi(t)\rangle_I$) are determined by their respective equations of motions. These are

$$\frac{\partial |\psi(t)\rangle_I}{\partial t} = -i\hat{V}_I(t)|\psi(t)\rangle_I \quad \& \quad \frac{\partial |\psi(t)\rangle_S}{\partial t} = -i\hat{H}(t)|\psi(t)\rangle_S; \tag{3.5}$$

for a Hamiltonian in the form of $\hat{H}(t) = \hat{H}_o + \hat{V}(t)$. Within the Interaction picture $\hat{V}_I(t) = e^{i\hat{H}_o t}\hat{V}(t)e^{-i\hat{H}_o t}$.

It is important to notice that any state ket can be transformed from the Schrödinger picture to the Interaction picture via $|\psi(t)\rangle_I = e^{i\hat{H}_o t}|\psi(t)\rangle_S$. This means that the density of

Figure 3.11: Numerically evaluating $\mathcal{D}_{F;I}(t)$ directly through the dynamic fidelity in the Interaction picture (Eq. 2.24) along with the QFI in the Interaction picture $2\mathrm{Var}[\hat{V}_I(t)]_I$ (Eq. 2.29) and the QFI in the Schrödinger picture $\mathrm{Var}[\hat{H} - \hat{H}_o]_S$ (Eq. 2.28) for the BJJ-impurity system at $N = 10$, and $v = 0.01$. Each of these lines overlap with one another concluding that the QFI in the Interaction picture is equivalent to its Schrödinger picture form, along with the DFS in the Interaction picture.

defects ($n_{ex}(t) = P_{ex}(t) = 1 \quad jh \quad (t)jE_0(vt)ij^2$) should be the same in both pictures. Using this model to directly calculate Eq. (2.24) through the dynamic delity $jh \ (t)j_I \ (t + \ t)i_I j$, we can see how the analytic relations give by (Eqs. 2.29 and 2.28) compare in Figure 3.11. Numerically, the results seem identical to the analytic results derived and show consistency between the expressions written in the Schrodinger picture and the Interaction picture. This means that any connections found within the Schrodinger picture can be extended to the Interaction picture through simple relations!

Finally, we express DFS for this model in its FOTOC equivalent given by Eq. (2.41) in Figure 3.12. Additionally we plot out the traditional FOTOC given by Eq. (2.36) to compare and contrast directly. What we see is that the assumptions are necessary to arrive at the nal result given by Eq. (2.40). This equivalence provides a way to interpret how OTOCs behave for systems within the context of slow driving protocols. Due to the numeric dif culty in calculating OTOCs directly [38], this could provide a new avenue towards numerically calculating OTOCs in a similar manner. Optimistically, this equivalence could lead to a possible connection between quantum scrambling and the dynamics of QPT's [77, 78].

Figure 3.12: Dynamic delity susceptibility (DFS) is evaluated through the dynamic delity $jh \ (t)j_{l} \ (t + \ t)i_{l}j$ by Eq. (2.24) and it is compared to the FOTOC ($jh \ (0)j_{l} \hat{W}^{y}_{G}(t)j \ (0)i_{l}j^{2}$ where $W_{V(t)}(t; \ t) = e^{j \ t \ \hat{V}(t)}$) from Eq. (2.32) along with the OTOC represented form for DFS ($2\frac{(1 \ jh \ (t)j_{l} \hat{W}^{y}_{G}(t)j \ (t)i_{l}j^{2})}{(\ t)^{2}}$) as illustrated in Eq. (2.41). The results in this graph are for the BJJ-impurity system when it is evaluated at $N = 10$, and $v = 0:01$ (an adiabatic speed for $N = 10$) for a linear driving protocol de ned by Eq. (3.4). This gure shows how DFS is extended from the traditional FOTOC as de ned in Eq. (2.36) and how it is written as an OTOC since the green and yellow lines are directly overlapping. This connection provides a clear description to the behaviour of OTOC's in a slow driving protocol! Further exploration of this concept could describe possible connections between the dynamics of OTOC's and the dynamics of QPT's [77, 78]

Chapter 4

Future work

Given the intimate relationship between generalized fidelity susceptibility and the excitation probability, writing dynamic fidelity susceptibility (DFS) in an equivalent generalized form could lead to a direct connection between DFS and the density of defects [79]. DFS can be applied to quantum quenches starting in different many-body eigenstates to explore excited state quantum phase transitions [80]. Dynamic fidelity can be expanded up to higher order terms for the velocity or the wavefunction. Considering a non-linear time dependence could provide a general connection between DFS and fidelity susceptibility in the adiabatic limit. Further exploration on the connection between the dynamics of QPT's and OTOC's through DFS could be fruitfull [77, 78]. It would be interesting to see how DFS behaves for systems of other universality classes. One important application for this work would be in the field of quantum computation. The errors that accumulate within an adiabatic quantum computation process can be described by the density of defects about a quantum critical point [81]. Ultimately, deriving an analytic scaling laws for DFS would show how it can directly probe universal dynamics and why it would be the natural quantity to consider in the field of out-of-equilibrium dynamics. Having an appropriate scaling law for DFS about a QCP could provide the context for describing the accumulation of errors when measuring multipartite entanglement. These are just a few of the possibly limitless applications that DFS can have!

Chapter 5

Conclusion

Dynamic delity susceptibility (DFS) has been shown to be a unique quantity for time evolving closed quantum systems that connects concepts between multipartite entanglement (QFI), scrambling (OTOC's), and universal dynamics. Thinking about DFS as an equivalent quantity to the QFI provides a unique approach to understanding the universal dynamics of quantum phase transitions. Just as the density of defects is often regarded as a measure of scalable errors within adiabatic quantum computation [81], DFS provides a means towards numerically understanding errors accumulated in quamtum comptuation by measuring multipartite entanglement (QFI) under a linear slow quench [82]. Within the adiabatic limit, there are interesting parallels between DFS and delity susceptibility creating expected outcomes with experimental measurements of the QFI. Remarkably, these results are found for a fairly complicated system (the BJJ-impurity model) with a linear time dependent control parameter and they have provided insight into possible numeric scaling laws that can hold for long-range interacting models. Some of the derived properties have also been shown for the transverse eld Ising model. Overall, DFS is shown to be a promising new quantity within the eld of out-of-equilibrium quantum dynamics and could have potential applications into quantum computation and cold-atom physics.

Appendix A

Solving the BJJ-impurity time dependent dynamics numerically

We start by writing the Hamiltonian in terms of its individual matrix elements as

$$\begin{aligned}
\langle m', n'|\hat{H}|m, n\rangle = & \left(2\frac{W}{JN}\left(n - m\right) + \frac{a}{JN}\left(n + \frac{a}{J} - m\right)\right)\delta_{n',n}\delta_{m',m} \\
& \frac{1}{2N}\sqrt{(N+2-n)(N-2-n+2)}\,\delta_{n',n-1}\delta_{m',m} \\
& \frac{1}{2N}\sqrt{(N+2-n+2)(N-2-n)}\,\delta_{n',n+1}\delta_{m',m} \\
& \frac{J-a}{2J}\sqrt{(M+2-m)(M-2-m+2)}\,\delta_{n',n}\delta_{m',m-1} \\
& \frac{J-a}{2J}\sqrt{(M+2-m+2)(M-2-m)}\,\delta_{n',n}\delta_{m',m+1};
\end{aligned} \tag{A.1}$$

where each of the coef cients in front of the Kroenecker delta's are represented as

$$\begin{aligned}
Q_m(n) &= 2\frac{W}{JN}\left(n - m\right) + \frac{a}{JN}\left(n + \frac{a}{J} - m\right) \\
F_{-1}(n) &= \frac{1}{2N}\sqrt{(N+2-n)(N-2-n+2)} \\
F_{+1}(n) &= \frac{1}{2N}\sqrt{(N+2-n+2)(N-2-n)} \\
G_{-1}(m) &= \frac{J-a}{2J}\sqrt{(M+2-m)(M-2-m+2)} \\
G_{+1}(m) &= \frac{J-a}{2J}\sqrt{(M+2-m+2)(M-2-m)}:
\end{aligned} \tag{A.2}$$

Notice how each term does not depend on N meaning they are numerically reasonable to calculate.

The next step is to solve the wavefunction through the Schrödinger equation. An important thing to note is that we are assuming the system starts in the ground state $|E_0(0)\rangle$ and

it passes through the critical point $W_c = 2\sqrt{JJ^a}$. With the transformation described in Eq. (3.3), the critical point looses its dependence on N. Thus, the wavefunction in the Fock basis is

$$|\psi(t)\rangle = \sum_{n=-\frac{N}{2}}^{\frac{N}{2}} \sum_{m=-\frac{M}{2}}^{\frac{M}{2}} a_{n,m}(t)|n, m\rangle : \tag{A.3}$$

When we are solving the Schrodinger equation, the range in which time occurs needs to be taken into account. For a linear quench scheme given by $W = vt$, time needs to change based on the appropriate quench speeds. If $W \in [W_{min}; W_{max}]$, then $t \in [\frac{t_{min}}{v}; \frac{t_{max}}{v}]$ which tells us that the amount of time needed to solve the Schrodinger equation changes drastically. Regardless, the Schrodinger equation is written as

$$i\frac{d|\psi(t)\rangle}{dt} = \hat{H}(vt)|\psi(t)\rangle : \tag{A.4}$$

Writing this out explicitly with Eq. (A.3) and the notation brought up from Eq. (A.2) gives

$$\begin{aligned}\sum_{n,m} a'_{n,m}(t)|n, m\rangle = -i \sum_{n,m} & Q_m(n)a_{n,m}(t)|n, m\rangle \\ & + F_{+1}(n)a_{n,m}(t)|n-1, m\rangle \\ & + F_{-1}(n)a_{n,m}(t)|n+1, m\rangle \\ & \frac{J^a}{J}(a_{n,m}(t)|n, m+1\rangle + a_{n,m}(t)|n, m-1\rangle) :\end{aligned} \tag{A.5}$$

Here, the prime denotes the time derivative. It should be noted that the terms defined through $G_{-1}(m)$ are equal to $\frac{J^a}{J}$ in the Hamiltonian. From here, we can see what each term is equal to

$$\begin{aligned}a'_{n,m}(t) = -i\, & a_{n,m}(t)Q_m(n) + F_{+1}(n+1)a_{n+1,m}(t) \\ & + F_{-1}(n-1)a_{n-1,m}(t) - \frac{J^a}{J}(a_{n,m+1}(t) + a_{n,m-1}(t)) :\end{aligned} \tag{A.6}$$

These are the equations being solved for each of the coefficients of the wavefunction. As we can see, they are highly coupled with one another but fortunately have a limited time dependence. So when we are actually solving these coupled ODE's, we have to note the range in which time occurs. Given that the initial condition is $|\psi_0(t_o = 0)\rangle = |E_0(W = 0)\rangle$, we can solve Eq. (A.6).

Bibliography

[1] Mehran Kardar. Statistical physics of fields. Cambridge University Press, 2007.

[2] Subir Sachdev. Quantum phase transitions. Wiley Online Library, 2011.

[3] Anatoli Polkovnikov, Krishnendu Sengupta, Alessandro Silva, and Mukund Vengalattore. Colloquium: Nonequilibrium dynamics of closed interacting quantum systems. Reviews of Modern Physics, 83(3):863, 2011.

[4] Paul M Chaikin, Tom C Lubensky, and Thomas A Witten. Principles of condensed matter physics, volume 1. Cambridge university press Cambridge, 1995.

[5] Lei Wang, Ye-Hua Liu, Jakub Imriška, Ping Nang Ma, and Matthias Troyer. Fidelity susceptibility made simple: A unified quantum monte carlo approach. Physical Review X, 5(3):031007, 2015.

[6] Shi-Jian Gu. Fidelity approach to quantum phase transitions. International Journal of Modern Physics B, 24(23):4371–4458, 2010.

[7] A Fabricio Albuquerque, Fabien Alet, Clément Sire, and Sylvain Capponi. Quantum critical scaling of fidelity susceptibility. Physical Review B, 81(6):064418, 2010.

[8] Lorenzo Campos Venuti and Paolo Zanardi. Quantum critical scaling of the geometric tensors. Physical review letters, 99(9):095701, 2007.

[9] Michael A Nielsen and Isaac Chuang. Quantum computation and quantum information, 2002.

[10] Jens Eisert, Marcus Cramer, and Martin B Plenio. Colloquium: Area laws for the entanglement entropy. Reviews of Modern Physics, 82(1):277, 2010.

[11] Silvia Pappalardi, Angelo Russomanno, Alessandro Silva, and Rosario Fazio. Multipartite entanglement after a quantum quench. Journal of Statistical Mechanics: Theory and Experiment, 2017(5):053104, 2017.

[12] Markus Greiner, Olaf Mandel, Tilman Esslinger, Theodor W Hänsch, and Immanuel Bloch. Quantum phase transition from a superfluid to a mott insulator in a gas of ultracold atoms. *nature*, 415(6867):39–44, 2002.

[13] Andreas Osterloh, Luigi Amico, Giuseppe Falci, and Rosario Fazio. Scaling of entanglement close to a quantum phase transition. *Nature*, 416(6881):608, 2002.

[14] Mike H Anderson, Jason R Ensher, Michael R Matthews, Carl E Wieman, and Eric A Cornell. Observation of Bose-Einstein condensation in a dilute atomic vapor. In *Collected Papers Of Carl Wieman*, pages 453–456. World Scientific, 2008.

[15] Pierfrancesco Buonsante and Alessandro Vezzani. Ground-state fidelity and bipartite entanglement in the bose-hubbard model. *Physical review letters*, 98(11):110601, 2007.

[16] Wojciech H Zurek, Uwe Dorner, and Peter Zoller. Dynamics of a quantum phase transition. *Physical review letters*, 95(10):105701, 2005.

[17] Jacek Dziarmaga. Dynamics of a quantum phase transition: Exact solution of the quantum ising model. *Physical review letters*, 95(24):245701, 2005.

[18] Bogdan Damski and Wojciech H Zurek. Adiabatic-impulse approximation for avoided level crossings: From phase-transition dynamics to landau-zener evolutions and back again. *Physical Review A*, 73(6):063405, 2006.

[19] Anushya Chandran, Amir Erez, Steven S Gubser, and SL Sondhi. Kibble-zurek problem: Universality and the scaling limit. *Physical Review B*, 86(6):064304, 2012.

[20] Amit Dutta, Gabriel Aeppli, Bikas K Chakrabarti, Uma Divakaran, Thomas F Rosenbaum, and Diptiman Sen. *Quantum phase transitions in transverse field spin models: from statistical physics to quantum information*. Cambridge University Press, 2015.

[21] Clarence Zener. Non-adiabatic crossing of energy levels. *Proceedings of the Royal Society of London. Series A, Containing Papers of a Mathematical and Physical Character*, 137(833):696–702, 1932.

[22] Anatoli Polkovnikov and Vladimir Gritsev. Universal dynamics near quantum critical points. *Understanding Quantum Phase Transitions*, pages 59–90, 2011.

[23] X-L Deng, Diego Porras, and J Ignacio Cirac. Effective spin quantum phases in systems of trapped ions. *Physical Review A*, 72(6):063407, 2005.

[24] Nicolas Laflorencie, Ian Affleck, and Mona Berciu. Critical phenomena and quantum phase transition in long range heisenberg antiferromagnetic chains. *Journal of Statistical Mechanics: Theory and Experiment*, 2005(12):P12001, 2005.

[25] M Dalmonte, G Pupillo, and P Zoller. One-dimensional quantum liquids with power-law interactions: The luttinger staircase. *Physical review letters*, 105(14):140401, 2010.

[26] Zhangqi Zhu, Gaoyong Sun, Wen-Long You, and Da-Ning Shi. Fidelity and criticality of a quantum ising chain with long-range interactions. *Physical Review A*, 98(2):023607, 2018.

[27] Daniel Jaschke, Kenji Maeda, Joseph D Whalen, Michael L Wall, and Lincoln D Carr. Critical phenomena and kibble–zurek scaling in the long-range quantum ising chain. *New Journal of Physics*, 19(3):033032, 2017.

[28] Ming Xue, Shuai Yin, and Li You. Universal driven critical dynamics across a quantum phase transition in ferromagnetic spinor atomic bose-einstein condensates. *arXiv preprint arXiv:1805.02174*, 2018.

[29] Nicolò Defenu, Tilman Enss, Michael Kastner, and Giovanna Morigi. Dynamical critical scaling of long-range interacting quantum magnets. *Physical review letters*, 121(24):240403, 2018.

[30] Ricardo Puebla, Oliver Marty, and Martin B Plenio. Quantum kibble-zurek physics in long-range transverse-field ising models. *arXiv preprint arXiv:1906.04872*, 2019.

[31] Manuel Gessner and Augusto Smerzi. Statistical speed of quantum states: Generalized quantum fisher information and schatten speed. *Physical Review A*, 97(2):022109, 2018.

[32] Philipp Hauke, Markus Heyl, Luca Tagliacozzo, and Peter Zoller. Measuring multipartite entanglement through dynamic susceptibilities. *Nature Physics*, 12(8):778, 2016.

[33] Marco Gabbrielli, Augusto Smerzi, and Luca Pezzè. Multipartite entanglement at finite temperature. *Scientific reports*, 8(1):15663, 2018.

[34] Gabriele De Chiara and Anna Sanpera. Genuine quantum correlations in quantum many-body systems: a review of recent progress. *Reports on Progress in Physics*, 81(7):074002, 2018.

[35] Brian Swingle, Gregory Bentsen, Monika Schleier-Smith, and Patrick Hayden. Measuring the scrambling of quantum information. *Physical Review A*, 94(4):040302, 2016.

[36] Pavan Hosur, Xiao-Liang Qi, Daniel A Roberts, and Beni Yoshida. Chaos in quantum channels. *Journal of High Energy Physics*, 2016(2):4, 2016.

[37] Stephen H Shenker and Douglas Stanford. Black holes and the butterfly effect. *Journal of High Energy Physics*, 2014(3):67, 2014.

[38] RJ Lewis-Swan, A Safavi-Naini, JJ Bollinger, and AM Rey. Unifying scrambling, thermalization and entanglement through measurement of fidelity out-of-time-order correlators in the dicke model. *Nature communications*, 10(1):1581, 2019.

[39] Juan Maldacena, Stephen H Shenker, and Douglas Stanford. A bound on chaos. *Journal of High Energy Physics*, 2016(8):106, 2016.

[40] Kevin A Landsman, Caroline Figgatt, Thomas Schuster, Norbert M Linke, Beni Yoshida, Norman Y Yao, and Christopher Monroe. Verified quantum information scrambling. *Nature*, 567(7746):61, 2019.

[41] Martin Gärttner, Justin G Bohnet, Arghavan Safavi-Naini, Michael L Wall, John J Bollinger, and Ana Maria Rey. Measuring out-of-time-order correlations and multiple quantum spectra in a trapped-ion quantum magnet. *Nature Physics*, 13(8):781, 2017.

[42] Henk TC Stoof, Koos B Gubbels, and Dennis Dickerscheid. *Ultracold Quantum Fields*. Springer, 2009.

[43] Lev Davidovich Landau. On the theory of phase transitions. *Ukr. J. Phys.*, 11:19–32, 1937.

[44] Kerson Huang. *Introduction to statistical physics*. CRC press, 2009.

[45] B. Widom. Scaling laws. *Scholarpedia*, 4(10):9054, 2009. revision #91749.

[46] Jesse Mumford. *Singularities in a BEC in a double well potential*. PhD thesis, 2017.

[47] John Cardy. *Finite-size scaling*, volume 2. Elsevier, 2012.

[48] Wyatt Kirkby. *Singularities in Many-Body Quantum Dynamics*. PhD thesis, 2017.

[49] Jesse Mumford. Singularities in a BEC in a double well potential, 2017.

[50] Bogdan Damski. Fidelity approach to quantum phase transitions in quantum ising model. In *Quantum Criticality in Condensed Matter: Phenomena, Materials and Ideas in Theory and Experiment*, pages 159–182. World Scientific, 2016.

[51] C De Grandi, V Gritsev, and A Polkovnikov. Quench dynamics near a quantum critical point: Application to the sine-gordon model. *Physical Review B*, 81(22):224301, 2010.

[52] Luca Pezzè, Marco Gabbrielli, Luca Lepori, and Augusto Smerzi. Multipartite entanglement in topological quantum phases. *Physical review letters*, 119(25):250401, 2017.

[53] Yu-Ran Zhang, Yu Zeng, Heng Fan, JQ You, and Franco Nori. Characterization of topological states via dual multipartite entanglement. *Physical review letters*, 120(25):250501, 2018.

[54] Philipp Hyllus, Wiesław Laskowski, Roland Krischek, Christian Schwemmer, Witlef Wieczorek, Harald Weinfurter, Luca Pezzé, and Augusto Smerzi. Fisher information and multiparticle entanglement. *Physical Review A*, 85(2):022321, 2012.

[55] BM Escher, RL de Matos Filho, and L Davidovich. General framework for estimating the ultimate precision limit in noisy quantum-enhanced metrology. *Nature Physics*, 7(5):406, 2011.

[56] Paolo Zanardi, Paolo Giorda, and Marco Cozzini. Information-theoretic differential geometry of quantum phase transitions. *Physical review letters*, 99(10):100603, 2007.

[57] Helmut Strobel, Wolfgang Muessel, Daniel Linnemann, Tilman Zibold, David B Hume, Luca Pezzè, Augusto Smerzi, and Markus K Oberthaler. Fisher information and entanglement of non-gaussian spin states. *Science*, 345(6195):424–427, 2014.

[58] Pasquale Calabrese and John Cardy. Quantum quenches in extended systems. *Journal of Statistical Mechanics: Theory and Experiment*, 2007(06):P06008, 2007.

[59] Stefan Trotzky, Yu-Ao Chen, Andreas Flesch, Ian P McCulloch, Ulrich Schollwöck, Jens Eisert, and Immanuel Bloch. Probing the relaxation towards equilibrium in an isolated strongly correlated one-dimensional bose gas. *Nature Physics*, 8(4):325, 2012.

[60] Pasquale Calabrese, Fabian HL Essler, and Maurizio Fagotti. Quantum quench in the transverse-field ising chain. *Physical review letters*, 106(22):227203, 2011.

[61] Edward Farhi, Jeffrey Goldstone, Sam Gutmann, and Michael Sipser. Quantum computation by adiabatic evolution. *arXiv preprint quant-ph/0001106*, 2000.

[62] Jun John Sakurai, Jim Napolitano, et al. *Modern quantum mechanics*, volume 185. Pearson Harlow, 2014.

[63] Anatoli Polkovnikov. Universal adiabatic dynamics in the vicinity of a quantum critical point. *Physical Review B*, 72(16):161201, 2005.

[64] Amit Dutta, Gabriel Aeppli, Bikas K Chakrabarti, Uma Divakaran, Thomas F Rosenbaum, and Diptiman Sen. *Quantum Phase Transitions in Transverse Field Spin Models: From Statistical Physics to Quantum Information*. Cambridge University Press, 2015.

[65] Thomas WB Kibble. Topology of cosmic domains and strings. *Journal of Physics A: Mathematical and General*, 9(8):1387, 1976.

[66] Wojciech H Zurek. Cosmological experiments in superfluid helium? *Nature*, 317(6037):505, 1985.

[67] Wojciech H Zurek. Cosmic strings in laboratory superfluids and the topological remnants of other phase transitions. *Acta Phys. Polon.*, 24:1301–1311, 1993.

[68] Bogdan Damski. The simplest quantum model supporting the kibble-zurek mechanism of topological defect production: Landau-zener transitions from a new perspective. *Physical review letters*, 95(3):035701, 2005.

[69] Markus Schmitt, Dries Sels, Stefan Kehrein, and Anatoli Polkovnikov. Semiclassical echo dynamics in the sachdev-ye-kitaev model. *Physical Review B*, 99(13):134301, 2019.

[70] Barry M Garraway. The dicke model in quantum optics: Dicke model revisited. *Philosophical Transactions of the Royal Society A: Mathematical, Physical and Engineering Sciences*, 369(1939):1137–1155, 2011.

[71] Anna Francuz, Jacek Dziarmaga, Bartłomiej Gardas, and Wojciech H Zurek. Space and time renormalization in phase transition dynamics. *Physical Review B*, 93(7):075134, 2016.

[72] F Mulansky, J Mumford, and DHJ O'Dell. Impurity in a Bose-Einstein condensate in a double well. *Physical Review A*, 84(6):063602, 2011.

[73] M Rinck and C Bruder. Effects of a single fermion in a bose josephson junction. *Physical Review A*, 83(2):023608, 2011.

[74] Jesse Mumford, Jonas Larson, and DHJ O'Dell. Impurity in a bosonic Josephson junction: Swallowtail loops, chaos, self-trapping, and dicke model. *Physical Review A*, 89(2):023620, 2014.

[75] Jesse Mumford and DHJ O'Dell. Critical exponents for an impurity in a bosonic Josephson junction: Position measurement as a phase transition. *Physical Review A*, 90(6):063617, 2014.

[76] T Zibold. T. zibold, e. nicklas, c. gross, and mk oberthaler, phys. rev. lett. 105, 204101 (2010). *Phys. Rev. Lett.*, 105:204101, 2010.

[77] Ceren B Dağ, Kai Sun, and L-M Duan. Detection of quantum phases via out-of-time-order correlators. *arXiv preprint arXiv:1902.05041*, 2019.

[78] Bo-Bo Wei, Gaoyong Sun, and Myung-Joong Hwang. Dynamical scaling laws of out-of-time-ordered correlators. *arXiv preprint arXiv:1906.00533*, 2019.

[79] Victor Mukherjee and Amit Dutta. Fidelity susceptibility and general quench near an anisotropic quantum critical point. *Physical Review B*, 83(21):214302, 2011.

[80] MA Caprio, P Cejnar, and F Iachello. Excited state quantum phase transitions in many-body systems. *Annals of Physics*, 323(5):1106–1135, 2008.

[81] Bartłomiej Gardas, Jacek Dziarmaga, Wojciech H Zurek, and Michael Zwolak. Defects in quantum computers. *Scientific reports*, 8(1):4539, 2018.

[82] K Wright, KM Beck, S Debnath, JM Amini, Y Nam, N Grzesiak, J-S Chen, NC Pisenti, M Chmielewski, C Collins, et al. Benchmarking an 11-qubit quantum computer. *arXiv preprint arXiv:1903.08181*, 2019.